nature communications

Article

https://doi.org/10.1038/s41467-024-50491-x

A synthetic peptide mimic kills *Candida albicans* and synergistically prevents infection

Received: 15 September 2023

Accepted: 11 July 2024

Published online: 09 August 2024

Check for updates

Sebastian Schaefer[1,2,3,4], Raghav Vij[4], Jakob L. Sprague[4], Sophie Austermeier[4], Hue Dinh[5], Peter R. Judzewitsch[1,2], Sven Müller-Loennies[6], Taynara Lopes Silva[7], Eric Seemann[8], Britta Qualmann[8], Christian Hertweck[7,9,10], Kirstin Scherlach[7], Thomas Gutsmann[6,11], Amy K. Cain[5], Nathaniel Corrigan[1,2], Mark S. Gresnigt[10,12], Cyrille Boyer[1,2] ✉, Megan D. Lenardon[3] ✉ & Sascha Brunke[4] ✉

More than two million people worldwide are affected by life-threatening, invasive fungal infections annually. *Candida* species are the most common cause of nosocomial, invasive fungal infections and are associated with mortality rates above 40%. Despite the increasing incidence of drug-resistance, the development of novel antifungal formulations has been limited. Here we investigate the antifungal mode of action and therapeutic potential of positively charged, synthetic peptide mimics to combat *Candida albicans* infections. Our data indicates that these synthetic polymers cause endoplasmic reticulum stress and affect protein glycosylation, a mode of action distinct from currently approved antifungal drugs. The most promising polymer composition damaged the mannan layer of the cell wall, with additional membrane-disrupting activity. The synergistic combination of the polymer with caspofungin prevented infection of human epithelial cells in vitro, improved fungal clearance by human macrophages, and significantly increased host survival in a *Galleria mellonella* model of systemic candidiasis. Additionally, prolonged exposure of *C. albicans* to the synergistic combination of polymer and caspofungin did not lead to the evolution of tolerant strains in vitro. Together, this work highlights the enormous potential of these synthetic peptide mimics to be used as novel antifungal formulations as well as adjunctive antifungal therapy.

Modern medicine often relies on invasive medical interventions or drugs which can compromise the patient's immune system. An unfortunate consequence of these undeniably successful treatments for life-threatening diseases like cancer is severe infections caused by opportunistic pathogens[1,2]. Among these opportunists are fungal pathogens, including *Candida*, *Aspergillus*, *Cryptococcus*, and *Pneumocystis* species[1–3]. More recently, increasing numbers of opportunistic fungal infections caused by *Aspergillus*, *Mucorales*, and *Candida* species have been observed in COVID-19 patients with severe respiratory syndromes in intensive care units[4]. These and other factors result in over 2 million invasive fungal infections annually worldwide, with alarmingly high mortality rates and more than 1.5 million deaths[3].

A full list of affiliations appears at the end of the paper. ✉e-mail: cboyer@unsw.edu.au; m.lenardon@unsw.edu.au; sascha.brunke@leibniz-hki.de

Candida spp. is the fourth most common cause of hospital-acquired infections, and mortality rates from systemic *Candida* infections exceed 40%, even with antifungal intervention[3,5]. Among all *Candida* species, *Candida albicans* accounts for around 50% of *Candida* bloodstream infections[3,6]. Novel pathogenic species, such as the multi-drug-resistant *Candida auris* have emerged, potentially through adaptations to higher ambient temperature due to global climate change[7,8]. Indeed, *C. auris* and *C. albicans* were listed as two of the four critical group pathogens in the World Health Organization's first-ever fungal priority pathogens list, emphasising the need for new treatment options[9].

There are currently only four classes of antifungal drugs approved for the treatment of invasive *Candida* infections – azoles (*e.g.*, fluconazole), polyenes (*e.g.*, amphotericin B), echinocandins (*e.g.*, caspofungin), and flucytosine[10]. Their application is limited by undesired drug-drug interactions (azoles), detrimental off-target side-effects (polyenes), and the increasing occurrence of drug resistance (azoles, flucytosine, and echinocandins)[10,11]. Resistance of *Candida* spp. occurs mainly due to target over-expression, modification of the drug target, or upregulation of drug-efflux pumps[11]. The urgency to find new treatment options against *Candida* spp. was highlighted by the Centers for Disease Control and Prevention's (CDC) 2019 classification of *Candida* spp. as a serious threat to human health with equal standing to multi-drug-resistant bacteria such as *Pseudomonas aeruginosa*[12]. However, discovering novel targets for antifungal drugs is complicated by the evolutionary similarity of eukaryotic human and fungal cells, and the antifungal development pipeline is dominated by compounds from established classes, which are likely to result in similar complications[10,13]. Exceptions are fosmanogepix and ibrexafungerp which are first-in-class and undergoing clinical trials[14,15], but ultimately the emergence of resistance and clinical success for these new classes remain to be seen[14]. Combination therapy can decrease the development of resistance or re-sensitise resistant strains by acting on multiple targets[16–18]. It can also reduce toxicity to the host by decreasing required drug concentrations[16].

In nature, antifungal peptides (AFPs) prevent and combat fungal infections in all domains of life[19]. Most interact with the fungal cell membrane, damaging the cell wall or membrane or causing intracellular stress[19]. Employing those potent natural effectors as a drug is hampered by several issues; the membrane-active AFPs are often toxic to the expression host in biotechnological synthesis, chemical synthesis of peptides is expensive and complicated by their sequence specificity, and susceptibility to host proteases generally limits the applicability of AFPs[19]. These issues can be circumvented by mimicking cationic amphiphilic properties of AFPs synthetically[20,21]. Various polymeric synthetic structures show promising antifungal properties, including β-peptides[22,23], poly(2-oxazoline)s[24,25], polycarbonates[26], polyacrylamides[27,28], and peptidopolysaccharides[29]. Owing to advances in polymerisation techniques, particularly reversible-deactivation radical polymerisation (RDRP), synthetic macromolecules can be produced in a facile manner with precise control over molecular weight and composition[30]. However, one of the remaining challenges for RDRP is the synthesis of strictly homogeneous sequence-defined molecules, which would resemble AFPs with precisely defined sequences[31]. Due to this limitation, synthetic copolymers are usually synthesised with statistically distributed monomers or as a block copolymer, which to a certain degree provide control over sequence and dispersity[31].

Our group previously synthesised and screened a library of synthetic polyacrylamides inspired by AFP structures for activity against *C. albicans* and biocompatibility[27]. We identified polymers that outperformed amphotericin B in terms of their therapeutic index against *C. albicans* in vitro[27]. In the current work, we determined the mode of action of our most promising polymer compositions and investigated the in vitro and in vivo therapeutic potential of synergistic combinations of our polymers with existing antifungals with a view to enhancing efficacy, minimising toxicity and preventing the emergence of antifungal drug resistance.

Results and discussion

Synthesis and characterisation of amphiphilic polyacrylamides that mimic AFPs

Inspired by the physicochemical properties of antimicrobial peptides, we previously synthesised random acrylamide copolymers using photo-induced reversible-deactivation radical polymerisation[27,30]. The polymer characteristics that conferred the highest activity against *C. albicans* and best biocompatibility with mammalian host cells (measured by in vitro therapeutic indexes) were short polymers with a degree of polymerisation (X_n) of 20 and an optimal balance of hydrophilic to hydrophobic groups[27]. Here, we synthesised four ternary polyacrylamides with these characteristics (Fig. 1 and Table 1), which previously demonstrated the most promising properties: LP (linear, pentyl), LH (linear, heptyl), CB (cyclic, benzyl), and CX (cyclic, hexyl), named by their distinct hydrophobic features. The successful synthesis and purification were confirmed by ^{1}H nuclear magnetic resonance (NMR) spectroscopy and refractive index-based size-exclusion chromatography (SEC). We achieved nearly complete monomer conversion of >98% and observed narrow, unimodal molecular weight distributions with a dispersity ($Đ$) between 1.09 and 1.12 (Supplementary Figs. S1-S15).

Polyacrylamides are active against drug-resistant, clinical *C. albicans* isolates

Our previous work showed that our polymers were active against *C. albicans* and other ascomycetes including *Candida glabrata* (*Nakaseomyces glabratus*), *Candida krusei* (*Pichia kudriavzevii*), and *Saccharomyces cerevisiae*, as well as the basidiomycete *Cryptococcus neoformans*[27]. Despite a high tolerance of *C. neoformans* towards AmpB and fluconazole, and intrinsic resistance of *S. cerevisiae* and *C. glabrata* towards fluconazole, all were susceptible to the four candidate polymers[27]. This suggested a mode of action that is different to AmpB and fluconazole. To explore this further, the minimum inhibitory concentration (MIC, growth inhibition of >90% at 24 h) of the polymers against antifungal drug-resistant strains of *C. albicans* (Table 2) was

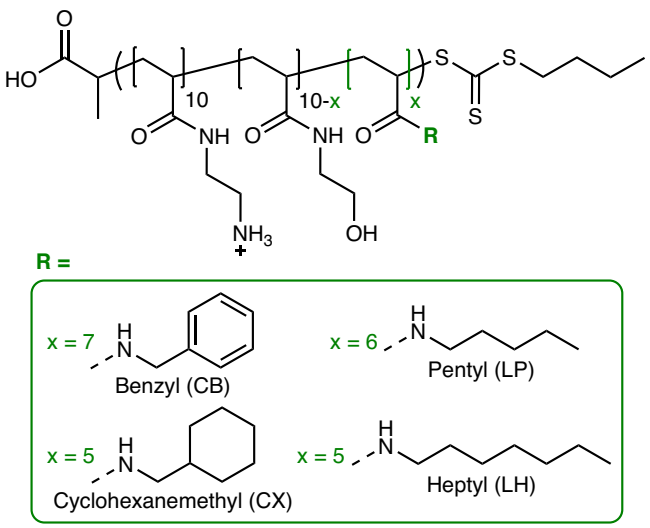

Fig. 1 | Chemical structures of polyacrylamides synthesised for this study. R represents the different side chains and x indicates the targeted number of hydrophobic residues within the molecule.

Table 1 | Composition, targeted degree of polymerisation (X_n), calculated molecular weight (M), experimental number-average molecular weight (M_n) and dispersity ($Đ$) of polymers employed in this study

Polymer	Targeted polymer composition (% positively charged/hydrophilic/hydrophobic functionality)	Experimental polymer composition (% positively charged/hydrophilic/hydrophobic functionality)[a]	Targeted X_n	Calculated M (g/mol) [b]	M_n (g/mol) [c]	$Đ$ [c]
LP	50/20/30	50/21/29	20	3700	6300	1.12
LH	50/25/25	50/25/25	20	3800	6400	1.09
CB	50/15/35	50/15/35	20	3900	6600	1.10
CX	50/25/25	49/26/25	20	3800	6100	1.09

[a]determined by ^{1}H NMR spectroscopy before polymerisation.
[b]calculated by ChemDraw (version 19.0) for Boc-protected polymers based on targeted composition and X_n, rounded to the nearest 100.
[c]determined by SEC using poly(methyl methacrylate) standards.

assessed using slightly modified Clinical and Laboratory Standards Institute (CLSI) guidelines[32,33].

C. albicans strain 110.12 is resistant to azoles and caspofungin, the latter due to a mutation in the echinocandin target Gsc1, an essential β-1,3-glucan synthase subunit[34]. The MICs for the polymers LP, CB and CX were only slightly increased compared to wild type, and the clinical isolate was at least as susceptible as the wild type to polymer LH.

AmpB-tolerant (EU0108, EU1008) or -resistant (EU0012, EU0136) strains have various mutations in enzymes involved in the biosynthesis of ergosterol (Erg3, Erg5, Erg6, Erg11), the target of AmpB[35,36]. The strains are also azole-resistant, which has been attributed to increased drug efflux at least in strain EU0108[35,36]. However, all polymers were active against those clinical isolates with even decreased MICs against the AmpB-tolerant strains. LH was fully active against the AmpB-resistant strains. A slight increase in MIC was observed for LP, CB, and CX.

The fluconazole-resistant *C. albicans* strains EU0992 and EU0989 have an increased Cdr-mediated drug efflux, and EU0981 and EU0999 show more Mdr-dependent export activity, while all these strains are normal in sterol biosynthesis (O. Bader, personal communications)[37]. The antifungal activity of the polymers was not affected by those mutations, suggesting that they are not transported out by Cdr- or Mdr-related efflux pumps.

Comparing the MICs of the most active antifungal polymer LH against *C. albicans* (8–32 μg/mL, 3–11 μM) to reported MICs of antimicrobial peptides reveals them to be active at similar concentrations. For example, the membrane-lytic peptides LL-37 (human) and melittin (bee venom) inhibit *C. albicans* growth at concentrations of 64 μg/mL (14 μM) and 11–22 μg/mL (4–8 μM), respectively[38,39], while the intracellularly acting histatin 5 (human) exhibited slightly lower MICs against *C. albicans* (4–8 μg/mL, 3–5 μM)[40,41]. Some synthetic cationic peptides composed of 9–11 amino acids have shown MICs against *C. albicans* in an equivalent range of 8–32 μg/mL (6–23 μM) and also interfere with fungal membranes[42,43].

Overall, each antifungal drug-resistant *C. albicans* strain tested was as susceptible to polymer LH, if not more, as the wild type. This indicates a distinct mode of action of LH. The different activity pattern of the other polymers against drug-resistant strains may indicate slight differences in modes of action between the polymers. We therefore investigated the potentially novel modes of action of our polymers.

Transcript profiling to investigate the mode of action of the antifungal polymers

We compared the transcriptome of *C. albicans* cells grown for 1 h in the presence of sub-inhibitory concentrations of the antifungal polymers to untreated control. A non-active polymer, poly(hydroxyethyl acrylamide) (poly-HEA), was also included for comparison (chemical characterisation for poly-HEA in Supplementary Figs. S14 and 15 and Table S1) as well as the membrane-active antimicrobial peptide LL-37[38,44].

An overview of the global transcriptomic differences of *C. albicans* in response to the polymers and LL-37 was gained through hierarchical clustering and principal component analyses of normalised gene expression data. These analyses showed that the transcriptome of cells exposed to the antifungal polymers LP, CB, and CX clustered together (Supplementary Fig. S16). Surprisingly, the hierarchical clustering revealed that the transcriptomic patterns for these three polymers were more similar to the non-toxic poly-HEA (Supplementary Fig. S16A), while our most active candidate LH clustered separately after applying either of the two statistical methods (Supplementary Fig. S16A, B). The antimicrobial peptide LL-37 clustered separately from all polymers.

Next, we looked for biological functions and pathways where there was an overrepresentation of up- or downregulated genes associated with the function or pathway in the datasets by performing Gene Ontology (GO) term[45] and Kyoto Encyclopedia of Genes and Genomes (KEGG) pathway enrichment[46] analyses (Fig. 2). Similar to our clustering analyses, we noted that the non-toxic poly-HEA differed from the four antifungal polymers and that among the polymers, LH showed the most distinct pattern with the highest number of differentially expressed genes. Therefore, we focussed our studies on the effect of polymer LH on *C. albicans* since it demonstrated the best activity against clinical *C. albicans* isolates in comparison to the other three polymers (Table 2) and triggered a distinct transcriptomic response in *C. albicans* (Fig. 2 and Supplementary Fig. S16) in the present study. Additionally, a previous study highlighted the potential of polymer LH due to its superior antifungal activity while showing comparatively low damage to red blood cells and murine fibroblasts[27].

Functional GO term enrichment with the GO term finder tool at *Candida* Genome Database[45] (Fig. 2A) and KEGG pathway enrichment analyses[46,47] (Fig. 2B) were performed on the sets of differentially expressed genes. Both analyses indicated that the amphiphilic antifungal polymers caused damage to the cell membrane and cell wall, leading to the metabolic arrest of *C. albicans*. GO terms associated with transporter activity were enriched in the downregulated gene set, indicating general stress and metabolic arrest of the cells (Fig. 2A). More specifically, oligopeptide transmembrane transporter activity was enriched in the set of genes downregulated following treatment with LH. Together with the overrepresentation of genes involved in lipid and protein binding, this supports the hypothesis of *C. albicans* sensing a toxic, peptide-like structure with amphiphilic properties. The KEGG pathway mitogen-activated protein kinase (MAPK) stress response was overrepresented in upregulated genes upon treatment with the antifungal polymers (Fig. 2B and Supplementary Fig. S17 after treatment with polymer LH). An upregulation of genes in the MAPK signalling pathway is typical for cell wall and osmotic stress or starvation and leads to cell cycle arrest and cell wall remodelling[48,49]. The metabolic arrest of the fungal cells was further indicated by the enrichment of the KEGG pathways ribosome, biosynthesis of amino

https://doi.org/10.1038/s41467-024-50491-x

Table 2 | Antifungal activity of polymers and selected antifungal drugs against *C. albicans* clinical isolates

C. albicans strain	Phenotype	Minimum inhibitory concentration$_{24h,\ 90\%}$ in µg/mL (µM)						
		Polymers				Antifungal drugs		
		LP	LH	CB	CX	AmpB	Flu	Cas
SC5314	Wild type	64–128 (24–47)	16–32 (6–11)	64 (22)	64 (23)	0.5–1 (0.5–1.1)	0.25–0.5 (0.8–1.6)	0.25–0.5 (0.2–0.5)
110.12	Gsc1-mutation	↑ 256 (95)	16 (6)	↑ 128 (44)	↑ 128 (46)	1–2 (1.1–2.2)	↑↑ >8 (>26)	↑↑ 4–8 (3.6–7.3)
EU0108	Erg11-/Erg5-mutation, enhanced Cdr-efflux	64 (24)	8–16 (3–6)	↓ 16–32 (6–11)	32–64 (11–23)	↑ 2 (2.2)	↑↑ >8 (>26)	0.5–1 (0.5–0.9)
EU0012	Erg3-mutation	128–256 (47–95)	16–32 (6–11)	64–128 (22–44)	64–128 (23–46)	↑↑ 2–4 (2.2–4.3)	↑↑ >8 (>26)	0.5–1 (0.5–0.9)
EU1008	Erg3-/Erg11-mutation	32–64 (12–24)	8–16 (3v6)	↓ 32 (11)	↓ 16–32 (6–11)	↑ 2 (2.2)	↑↑ >8 (>26)	0.5–1 (0.5–0.9)
EU0136	Erg6-deficient	↑ 256 (95)	16–32 (6–11)	↑ 128 (44)	64–128 (23–46)	↑↑ 4 (4.3)	↑↑ >8 (>26)	0.5 (0.5)
EU0992	Enhanced Cdr-efflux	64–128 (24–47)	16 (6)	64–128 (22–44)	64–128 (23–46)	1–2 (1.1–2.2)	↑↑ >8 (>26)	0.5–1 (0.5–0.9)
EU0989	Enhanced Cdr-efflux	128 (47)	8–16 (3–6)	64 (22)	64–128 (23–46)	1–2 (1.1–2.2)	↑↑ >8 (>26)	0.5–1 (0.5–0.9)
EU0981	Enhanced Mdr-efflux	64 (24)	8–16 (3–6)	64 (22)	32–64 (11–23)	1–2 (1.1–2.2)	↑↑ >8 (>26)	0.25–0.5 (0.2–0.5)
EU0999	Enhanced Mdr-efflux	64–128 (24–47)	8–16 (3–6)	64–128 (22–44)	32–64 (11–23)	1–2 (1.1–2.2)	↑↑ >8 (>26)	0.25–0.5 (0.2–0.5)

Minimum inhibitory concentrations were determined by the concentration at which the respective compound inhibited >90% of fungal growth compared to an untreated control after 24 h at 35 °C.
AmpB Amphotericin B, *Flu* Fluconazole, *Cas* Caspofungin.
↑↑ indicates resistance, ↑ indicates increased tolerance (up to two-fold increase in MIC), and ↓ indicates a decreased MIC compared to the wild type.

acids, and oxidative phosphorylation in the downregulated gene set upon treatment with the antifungal polymers.

Additionally, GO terms associated with glycosylation processes were enriched in the upregulated gene set, specifically hydrolase activity against *O*-glycosyl compounds and hexosyltransferase activity – a parental gene set of mannosyltransferase activity (Fig. 2A). Similarly, one significantly overrepresented KEGG pathway enriched in upregulated genes was protein processing in the endoplasmic reticulum (ER) (Fig. 2B). A more detailed look (Supplementary Fig. S18) revealed that *C. albicans* cells treated with LH strongly upregulated genes associated with glycosylation and ER-associated degradation of misfolded protein (ERAD), together suggesting a disruption in the correct glycosylation of proteins. In support of this hypothesis, we also observed upregulated genes in the *N*-glycan biosynthesis pathway (Supplementary Fig. S19).

GO terms relating to membrane stress were enriched in the upregulated gene set (Fig. 2A). This included calcium ion transmembrane transport, suggesting increased Ca^{2+} influx and membrane damage. KEGG pathway enrichment analysis also revealed a transcriptional signature expected from damage to the cell membrane (Fig. 2B), particularly with polymer LH. This includes an overrepresentation of glycosylphosphatidylinositol (GPI)-anchor biosynthesis and glycerolipid biosynthesis in the upregulated gene set, and steroid biosynthesis in the downregulated gene set.

In contrast, treatment with the non-toxic poly-HEA or the antimicrobial peptide LL-37 did not elicit a significant enrichment of these glycosylation-related GO terms and KEGG pathways. This shows that it is not a general response to the presence of polymers or to bioactive peptide(-like) substances. Instead, we found an enrichment of upregulated genes with GO terms associated with DNA, protein, and small molecule binding. This may indicate that *C. albicans* reacts to small, peptide(-like) molecules, however, they do not seem to influence glycosylated proteins.

We found nearly no KEGG pathways to be enriched for differentially regulated genes in the presence of poly-HEA. In the presence of LL-37, genes involved in MAPK signalling were significantly upregulated, indicating a fungal stress response to a toxic compound. Additionally, the KEGG pathways ribosome, biosynthesis of amino acids, and oxidative phosphorylation were significantly enriched in the downregulated gene set upon treatment with LL-37, indicating an expected metabolic arrest of the fungal cells. Those KEGG pathways were also overrepresented in the presence of the antifungal polymers, but not the non-toxic poly-HEA. Notably, genes in the KEGG pathway "protein processing in the ER" were specifically upregulated upon treatment with the antifungal polymers, but not poly-HEA or LL-37 (Fig. 2B and Supplementary Fig. S18, showing polymer LH vs. LL-37), again highlighting that ER protein processing and MAPK signalling responses are specific for polymers with antifungal activity. In addition, we found that the gene expression profiles of *C. albicans* exposed to our polymers are very distinct from published profiles under exposure to polyenes, azoles or echinocandins[50]. This again suggests a unique mode of action of our synthetic polymers.

Currently approved antifungals have specific cellular targets, and mutations in the affected enzymes are one of the main reasons for the development of resistance[10]. In contrast, antimicrobial peptides have multiple modes of action, decreasing the likelihood of the development of resistance[51]. For example, a *Musca domestica* (housefly) AFP triggers responses in *C. albicans* that include reaction to oxidative stress, cell wall and membrane maintenance, protein synthesis, and energy metabolism[52]. A bacterium-derived, membranolytic antifungal lipopeptide (jagaricin)[53] similarly induces a broad transcriptional response, comprising the upregulation of cell wall organisation/biogenesis and calcium ion transmembrane transport genes, and downregulation of transmembrane transport for substances such as oligopeptides[37]. Our antifungal polymers induced a similar transcriptional response in

https://doi.org/10.1038/s41467-024-50491-x

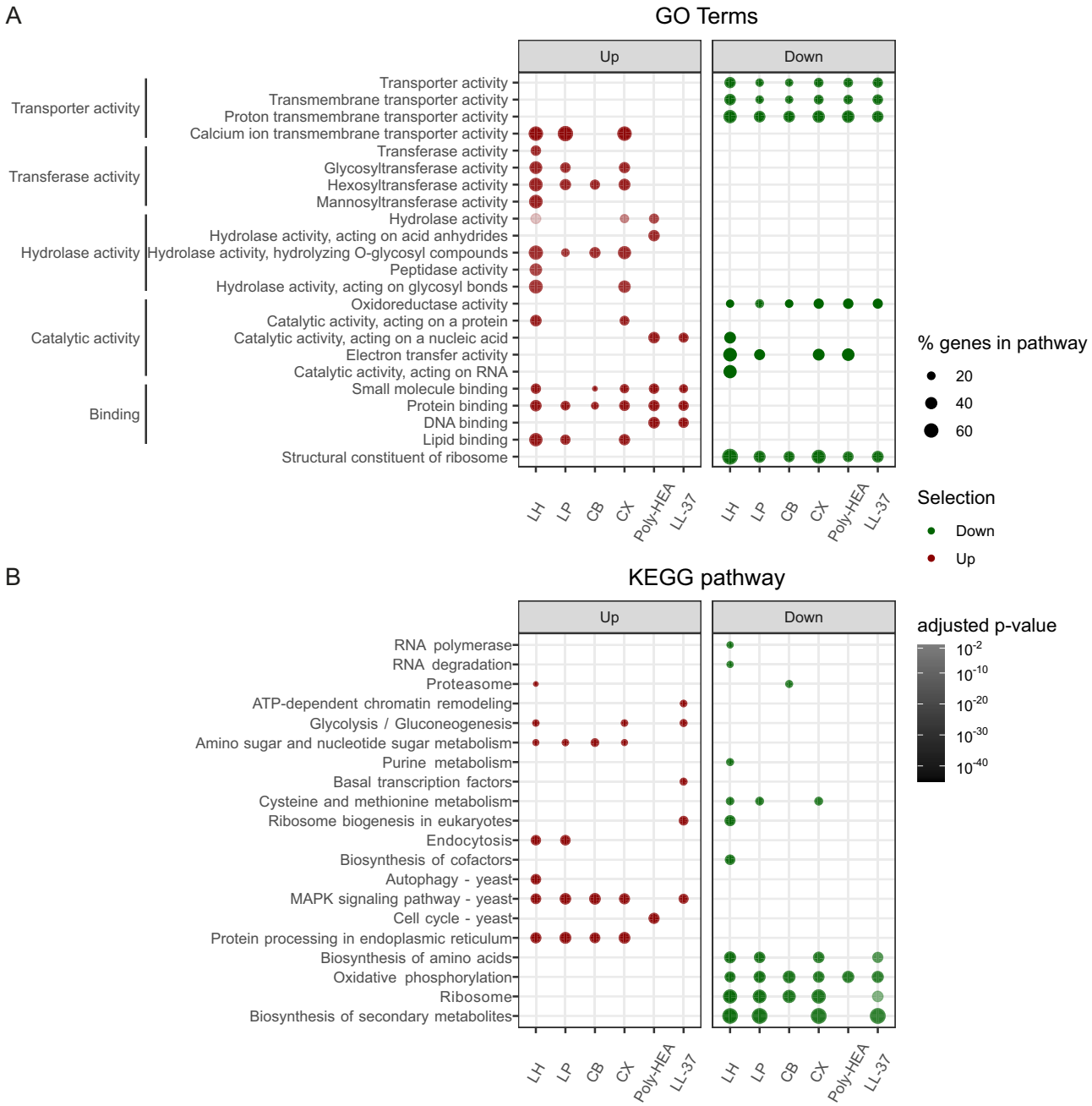

Fig. 2 | Antifungal polymers cause transcriptomic responses associated with impaired protein glycosylation, membrane stress, and cell wall damage in *C. albicans*. **A** Gene Ontology (GO) term enrichment analysis, based on molecular function[45], and **B** KEGG (Kyoto Encyclopedia of Genes and Genomes) pathway enrichment analysis[46] of RNA microarray data after treating *C. albicans* SC5314 for 1 h at 30 °C with sub-inhibitory concentrations of polymers and LL-37. Statistically significantly up- (red) or downregulated (green) gene groups associated with GO terms and KEGG pathways compared to the untreated control are shown. Diameter of circles reflects the percentage of genes differentially regulated in the associated pathway or term and the shading represents the adjusted *p*-value (calculated by hypergeometric distribution and adjusted by Benjamini–Hochberg correction for multiple testing). GO terms are additionally ordered by their assigned parental processes.

C. albicans. Altogether, these data led us to hypothesise that the antifungal polymers likely target multiple processes in *C. albicans* – they damage the cell wall and permeabilise the cell membrane, and they target protein glycosylation and thereby induce ER stress.

O-mannosylation, calcineurin, MAPK signalling, and a phosphoinositide regulator are required for *C. albicans* to survive polymer exposure

To gain further insights into the target of the polymers, we screened selected deletion mutants of *C. albicans* for their growth at sub-inhibitory polymer concentrations (LP, LH, CB, CX). Mutants were chosen to represent suspected target and resistance pathways, including cell wall organisation and stress response, membrane composition and inositol signalling, protein glycosylation (*O*- and *N*-linked mannosylation), calcineurin pathway, osmotic and oxidative stress response (MAPK signalling), drug efflux, and polyamine uptake (Supplementary Data S1). Growth curves were compared based on the time to reach half-maximal absorption (Supplementary Data S1). This growth speed index is positive for beneficial mutations (green shading in Supplementary Data S1) and

negative for detrimental ones (red shading in Supplementary Data S1).

The deletion of genes important for cell wall organisation and stress response had little effect on growth in the presence of polymers (Supplementary Data S1), with the exception of *ire1*, which showed no growth in the presence of LH. *IRE1* encodes a protein kinase of the unfolded protein response and cell wall organisation[54]. Interestingly, *IRE1* was also upregulated in the presence of LH (Supplementary Fig. S18).

Among the mutants for genes relevant to membrane composition and inositol signalling (Supplementary Data S1), *inp51* – lacking a phosphatase involved in the maintenance of phosphoinositide levels and thus cell wall and membrane integrity[55] – exhibited no growth in the presence of all polymers. *INP51* deletion has been shown to increase susceptibility to cell wall-active compounds[55]. The deletion of *ERG5*, involved in ergosterol biosynthesis, did not change the susceptibility to the polymers. This agrees well with the susceptibility of clinical AmpB-tolerant isolates towards the polymers (Table 2) and indicates that ergosterol biosynthesis likely does not affect the polymers' mode of action.

Deletion of genes contributing to *O*-linked protein mannosylation (*PMT1*, *PMT3*, *PMT4*, *PMT5*)[56] consistently increased susceptibility of *C. albicans* (Supplementary Data S1), suggesting that these activities are involved in the response to all antifungal polymers. In contrast, gene deletions affecting *N*-linked mannosylation (*MNN13*, *MNN14*, *MNN15*, *MNN22*, *MNN4*, *MNN9*, *MNS1*, *MNT4*, *OCH1*)[56] resulted in no change in susceptibilities.

Calcineurin and MAPK signalling are crucial in fungal development and response to environmental stress[57]. Two calcineurin pathway deletion mutants (*crz1*, *mid1*) showed no growth with normally sub-inhibitory polymer concentrations (Supplementary Data S1), and their genes' expression was also upregulated in *C. albicans* exposed to the antifungal polymers, but not poly-HEA. Two MAPK signalling deletion mutants (*hog1*, *pbs2*) also showed no growth in the presence of polymers. *HOG1* similarly has shown upregulation after exposure to the antifungal polymers, most prominently for LH and CX (Supplementary Fig. S17 for LH-treatment). Hence, the antifungal polymers seem to cause stress in *C. albicans*, and both calcineurin and MAPK pathways appear to be essential for fungal survival.

In agreement with the clinical drug-efflux mutants (Table 2), neither gain-of-function (in *MRR1* and *TAC1*) nor deletion (of *MRR1*, *SNQ2*, *TAC1*) of genes involved in drug efflux had a consistent impact on susceptibility.

The AFP histatin 5 is actively transported across the fungal membrane by polyamine transporters like Dur31 in *C. albicans* to exert its intracellular antifungal effect[58]. Our synthetic polymers share characteristics like cationic charge with both histatin 5 and polyamines, and their presence led to the upregulation of *DUR31*. However, deletion of *DUR31* or the related *DUR35*[59] resulted in a slightly increased (*dur31*) or unchanged susceptibility (*dur35*) (Supplementary Data S1), suggesting that the polymers are not primarily taken up by those transporters.

We also investigated selected *C. glabrata* (*Nakaseomyces glabratus*) mutants (marked blue in Supplementary Data S1). While none of the tested *C. albicans* mutations were beneficial, the deletion of *C. glabrata ERG5* and *INO2* increased tolerance to all antifungal polymers. Both genes are associated with membrane composition and inositol signalling. *C. glabrata cdr1*, lacking a drug-efflux pump-encoding gene, also showed increased growth with polymers, except LH. In contrast, deletion of *MNN2*, coding for an *N*-linked mannosyltransferase, had the highest benefit for LH-treated *C. glabrata* cells. Despite these slight differences, our data still suggests a very similar mode of action against *C. glabrata*. Like in *C. albicans*, deletion of genes encoding proteins involved in membrane composition and inositol signalling (*INP51*, *INP53*, *ISC1*), *O*-linked protein mannosylation (*PMT1*, *PMT2*) and MAPK signalling (*PBS2*) were more susceptible to the polymers, while the deletion of genes coding for proteins in the calcineurin pathway (*CNA1*, *CRZ1*, *MID1*) resulted in no growth in the presence of antifungal polymers.

In sum, the mutant screening agreed with our analyses of the transcriptome and suggested a mode of action connected to protein glycosylation and general stress of the polymers against *C. albicans*. Some similarities (involvement of MAPK and calcineurin signalling) were detected in a previous *C. albicans* mutant screen with the antifungal lipopeptide jagaricin, for which disruption of membrane integrity was suggested as the primary mode of action[37,53]. This suggests a similar effect of the synthetic polymers, especially as our gene expression analyses also showed possible interference with the plasma membrane (Fig. 2).

Polymer LH lyses *C. albicans* cell membranes

The polymers are inspired by antimicrobial peptides, which lyse bacterial and fungal membranes[60]. Membrane damage by the synthetic polymers was also suggested by gene expression analyses (Fig. 2) and mutant screening (Supplementary Data S1). We therefore investigated the membranolytic potential of polymer LH with a *C. albicans* strain constitutively expressing GFP in the cytosol (Fig. 3A–G). Two antifungal compounds were included – AmpB, which has membranolytic activity[61,62], and tunicamycin, which inhibits *N*-glycosylation of proteins, leading to cell death without membrane lysis[63]. Additionally, tethered membranes isolated from *C. albicans* and erythrocytes were incubated with polymer LH and non-toxic poly-HEA to investigate their potential to lyse synthetic membranes (Fig. 3I, J).

Untreated *C. albicans*-GFP cells showed a prominent intracellular GFP signal (Fig. 3A), which was absent in AmpB-treated cells (Fig.3B, G) where only 0.3% were viable as determined *via* backplating (Fig. 3H). The loss of GFP signal was due to membrane lysis, and not cell death per se, as tunicamycin-treated cells showed a less prominent loss of intracellular GFP (Fig. 3C), even though only 3% of cells were viable. The polymer LH (Fig. 3D–F) led to membranolytic activity, as seen by GFP signal loss, in a concentration-dependent manner with a proportional decrease in cell viability (36% at 0.5× MIC, 3% at 1× MIC at the assay conditions). Interestingly, at concentrations below MIC, we observed cell aggregates, which suggest a change in the surface properties of *C. albicans* cells.

To confirm the permeabilisation of membranes by polymer LH as part of its mode of action against *C. albicans*, tethered membranes composed of lipid mixtures isolated from *C. albicans* yeast or hyphae, or from erythrocytes, were incubated with polymer LH (Fig. 3I) or non-toxic poly-HEA (Fig. 3J). Polymer LH led to a concentration-dependent increase in membrane conductance, indicating membrane permeabilisation by pore formation (Fig. 3I and Supplementary Fig. S20A). The increase in membrane conductance was highest in the case of lipids from *C. albicans* yeast (Fig. 3I, black) and weaker for those from *C. albicans* hyphae (grey). Membranes composed of erythrocyte lipids were more stable and showed lower conductance before the addition of polymer LH and also at low concentrations of polymer LH, compared to membranes composed of *C. albicans* membranes. In contrast to polymer LH, poly-HEA did not lead to an order of magnitude differences in membrane conductance when increasing its concentration in any of the three lipid mixtures (Fig. 3J), indicating no lytic effect. As a control, the same experiment was performed with antimicrobial peptide LL-37 (Supplementary Fig. S20B), for which membrane permeabilisation has been reported as the primary mode of action against *C. albicans*[38,44]. Like polymer LH, LL-37 permeabilised *C. albicans* membranes at a concentration of 8 μg/mL. However, it also strongly affected tethered membranes isolated from erythrocytes, indicating a lower selectivity of LL-37 compared to polymer LH.

https://doi.org/10.1038/s41467-024-50491-x

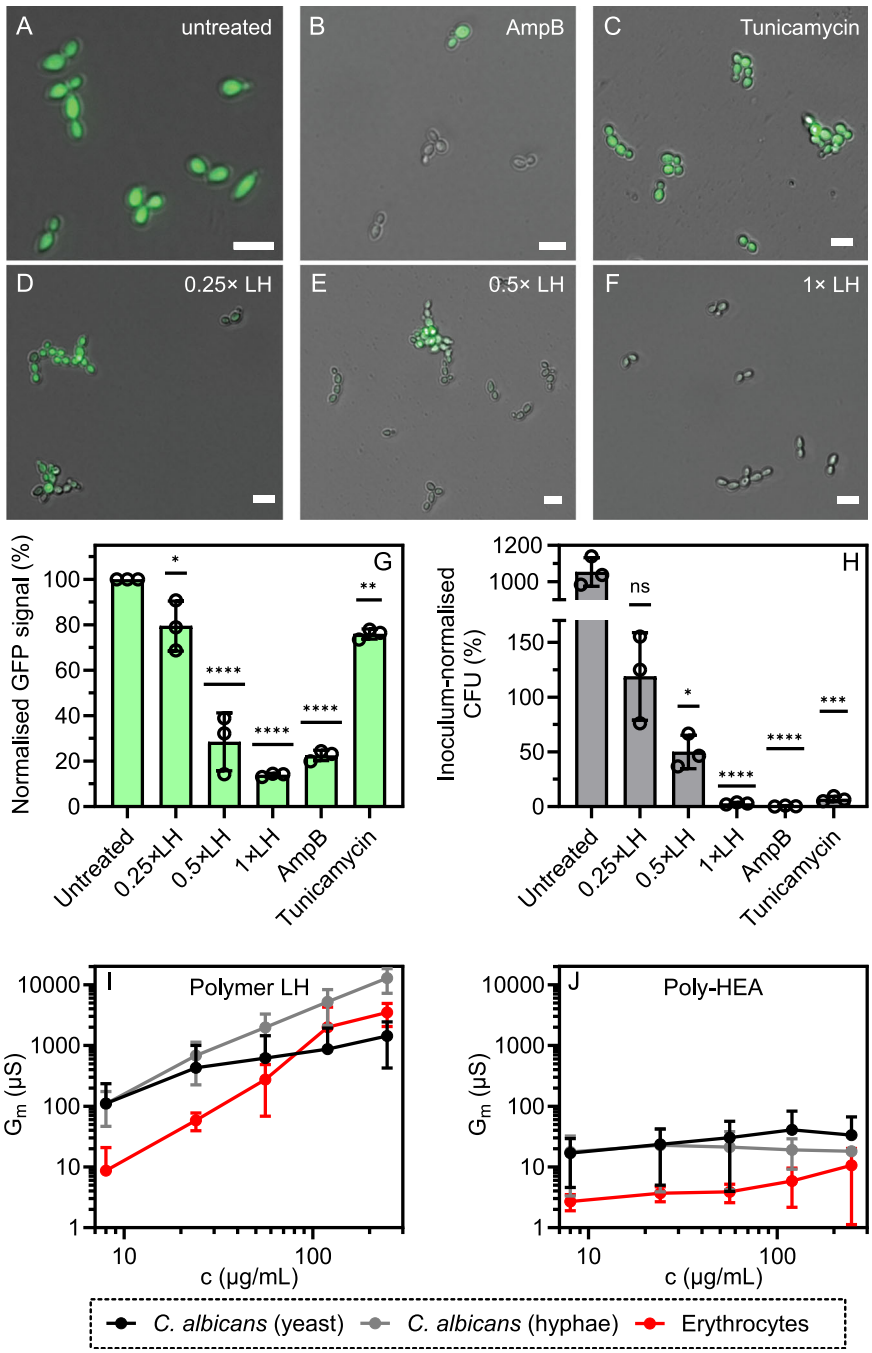

Fig. 3 | Polymer LH causes membrane lysis in *C. albicans*. Detection of fluorescence of *C. albicans* expressing cytoplasmic GFP (*ADH1*-GFP) after 6 h at MIC assay conditions for (**A**) untreated *C. albicans* cells, **B** cells treated with 1× MIC Amphotericin B (AmpB), **C** 1× MIC tunicamycin, **D** 0.25× MIC polymer LH, **E** 0.5× MIC polymer LH, and **F** 1× MIC polymer LH to investigate lytic activity of the compounds. Scale bars in (**A**–**F**) represent 10 µm. **G** The GFP signal was quantified from at least 50 *C. albicans*-GFP cells per biological replicate ($n = 3$), and then averaged and normalised to the respective untreated control. **H** Colony forming units (CFU) were determined by backplating and normalised to the inoculum ($n = 3$ biological replicates). Statistical significance in (**G**) and (**H**) was determined by Dunnett's ordinary one-way ANOVA multiple comparisons analysis (compared to untreated (100%) in (**G**) or inoculum (100%) in (**H**), $^{*}p < 0.05$ [**G**: $p = 0.0148$, **H**: $p = 0.0296$], $^{**}p < 0.01$ [**G**: $p = 0.0051$], $^{***}p < 0.0005$ [**H**: $p = 0.0002$], $^{****}p < 0.0001$) with ns indicating non-significant [**H**: $p = 0.4987$]. Average conductance (G_m) of tethered membranes isolated from *C. albicans* yeast (black) or hyphae (grey), or from erythrocytes (red) after the addition of increasing concentrations (**c**) of (**I**) antifungal polymer LH and (**J**) non-toxic poly-HEA in RPMI medium at 37 °C ($n = 3$ biological replicates). Error bars in (**G**–**J**) represent the standard deviation (SD) around the mean. Source data are provided as a Source Data file.

LH damages mannans attached to cell wall proteins, enhances phagocytosis, and affects yeast-to-hypha transition

Mutant screening and gene expression analyses suggested that glycosylated proteins might be primarily affected by the polymers. A major group of glycosylated proteins in *C. albicans* are the cell wall proteins. These are both *O*- and *N*-mannosylated as they pass through the ER and Golgi on their way to the wall. Once attached to the wall through GPI anchors or Pir linkages, the short *O*-mannan chains remain buried in the inner cell wall layer, whereas the long *N*-mannan chains protrude out from the cell surface forming an outer fibrillar layer of the cell wall (Fig. 4A)[64]. To investigate the effects of LH on the cell wall structure of *C. albicans*, fungal cells were incubated at sub-inhibitory

https://doi.org/10.1038/s41467-024-50491-x

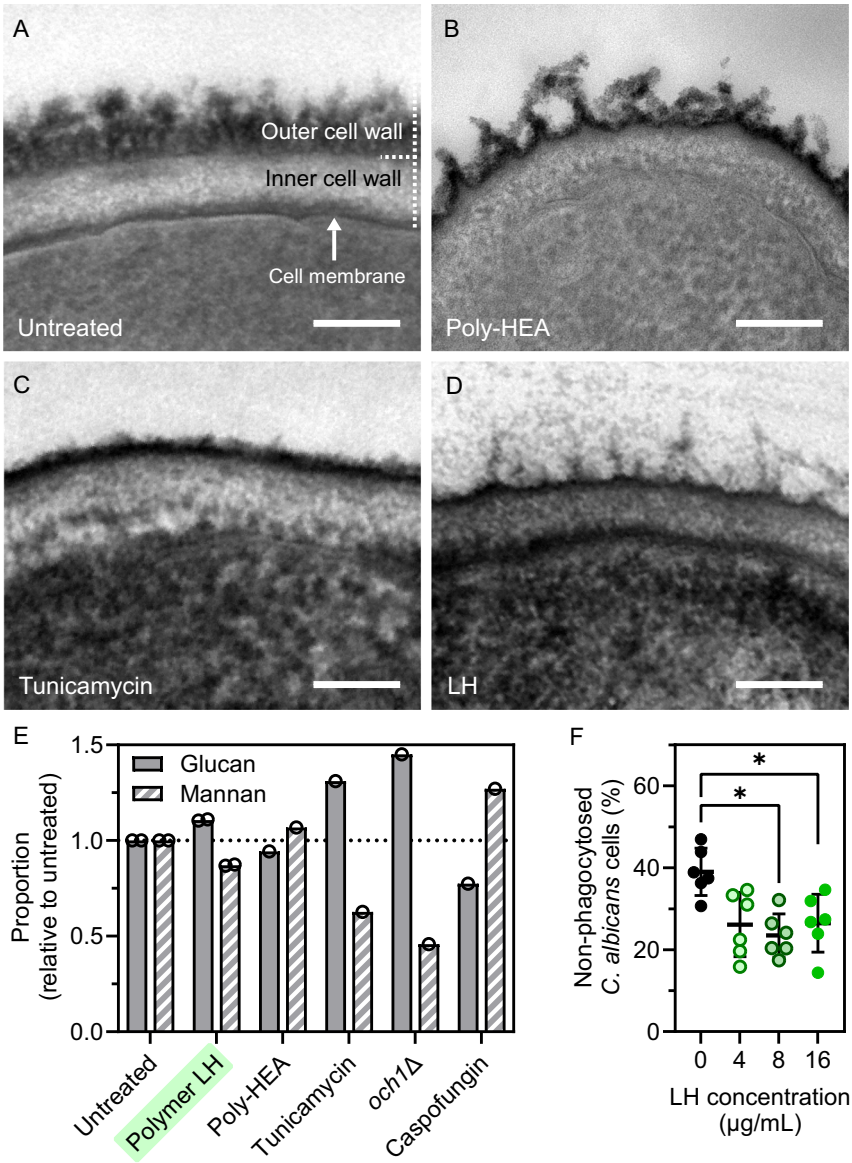

Fig. 4 | Cell wall changes in *C. albicans* and immune cell response to LH-treated *C. albicans*. Transmission electron microscopy (TEM) micrographs of the *C. albicans* cell wall after 6 h incubation in SD medium at 30 °C with (**A**) no additives, **B** with poly-HEA, **C** with tunicamycin, or **D** antifungal polymer LH, at sub-inhibitory concentrations of the antifungal compounds. The scale bars in (**A**–**D**) represent 100 nm. **E** The amount of glucan and mannan in cell walls isolated from *C. albicans* wildtype (SC5314) and *och1* mutant cells after 6 h of incubation in SD medium (untreated) and with sub-inhibitory concentrations of polymer LH, poly-HEA, tunicamycin, and caspofungin was determined by HPLC. Glucose (from glucan) and mannose (from mannan) represented 55% and 45% of the dry weight of the cell wall in wild-type untreated cells. The graph shows the proportions of glucan (grey bars) and mannan (striped bars) relative to those observed in untreated *C. albicans* wild-type cells. **F** Proportion of *C. albicans* cells not taken up over 15–30 min by human monocyte-derived macrophages. *C. albicans* cells were pre-treated with LH for one hour before putting them into contact with the macrophages ($n = 6$ biological replicates). Statistical significance in (**E**) was determined by Dunnett's repeated measures ANOVA multiple comparisons analysis (*$p < 0.05$ [0 vs 8 μg/ml: $p = 0.0173$; 0 vs 16 μg/ml; $p = 0.0192$]). Error bars in (**F**) represent the standard deviation (SD) around the mean. Source data are provided as a Source Data file.

concentrations for 6 h and analysed by transmission electron microscopy (TEM, Fig. 4A–D). Compared to the no-treatment control (Fig. 4A), treatment with the non-toxic poly-HEA resulted in no major ultrastructural changes to the cell wall (Fig. 4B). A reduction of the outer cell wall *N*-mannan layer was observed after treatment with tunicamycin, an inhibitor of *N*-glycosylation (Fig. 4C)[63]. Treatment with a sub-inhibitory concentration of LH (Fig. 4D) disrupted the arrangement of the *N*-mannan fibrils, supporting our transcriptome and mutant screen data. At these sub-inhibitory concentrations, LH did not cause any obvious disruption of the membrane.

To confirm the transcriptome and TEM observations quantitatively, cell walls from *C. albicans* were isolated after 6 h incubation, and after acid hydrolysis, mannose (from mannans) and glucose (from glucans) were separated and detected by high-performance liquid chromatography (HPLC) (Fig. 4E). Exemplary HPLC spectra are shown in Supplementary Fig. S21. In accordance with the TEM observations (Fig. 4D), treatment with sub-inhibitory concentrations of polymer LH decreased the proportion of mannan relative to untreated cells. In contrast, poly-HEA treatment had no effect on the relative proportion of glucan and mannan. Consistent with our observations in the TEM images (Fig. 4C), treatment with the *N*-glycosylation inhibitor tunicamycin reduced the mannan content relative to untreated cells. The proportion of mannan in *C. albicans och1* mutant cells was reduced relative to wild-type cells, as expected for an *N*-mannosylation mutant

and consistent with previous observations[62]. Finally, the β-glucan synthase-inhibiting antifungal drug caspofungin had the expected effect of decreasing the glucan and increasing mannan, relative to the untreated control[63]. Overall, our measurements were therefore in good agreement with the expected outcome four our controls and supported our notion of a defective protein glycosylation in *C. albicans* after treatment with polymer LH.

Components of the *C. albicans* cell wall are also recognised by innate immune cells[65]. We hypothesised that the LH-induced changes to the cell wall structure (Fig. 4D) could also impact immune recognition and clearance by human macrophages. To test this, we challenged *C. albicans* cells that were preincubated with or without polymer LH at sub-inhibitory concentrations with primary human monocyte-derived macrophages (hMDMs). Primary immune cells such as hMDMs show donor-dependent differences in their uptake efficiency. We therefore chose the time point (15 or 30 min) for each donor when 30–50% of untreated *C. albicans* cells were not yet phagocytosed by the specific macrophages. We found that LH pretreatment significantly increased clearance of *C. albicans* by primary hMDMs, even at sub-inhibitory concentrations between 4–16 μg/mL (Fig. 4F). Concentrations above 16 μg/mL of polymer LH, however, resulted in decreased clearance (Supplementary Fig. S22A). These are most likely due to toxic effects on the hMDMs, which became apparent at 128 μg/mL after 30 min (Supplementary Fig. S22B, measured by LDH release).

It has been previously reported that *C. albicans* mutants with *N*- or *O*-linked glycosylation defects are more efficiently phagocytosed than the wild type[66,67]. With our TEM, HPLC, and transcriptome data, this suggests that LH disrupts the mannan layer and induces cell wall remodelling which increases phagocytosis by macrophages. Thus, in vivo, the application of polymer LH could potentiate fungal clearance by innate immune cells.

The cytokine release by primary human peripheral blood mononuclear cells (PBMCs) to pre-treated *C. albicans* was characterised by the pro-inflammatory cytokines IL-1β, IL-6, and TNF (Supplementary Fig. S23). The increased clearance by hMDMs (Fig. 4F), was reflected by significantly decreased IL-1β, IL-6, and TNF responses of PBMCs at an LH concentration of 4 μg/mL (Supplementary Figs. S23). Higher LH concentrations resulted in no significant changes in the release of IL-1β and TNF and a significant increase of IL-6. The decrease in TNF agrees with previous observations on *C. albicans N*-mannosylation defective mutants with impaired recognition by immune cells[68,69]. As mannoproteins in *C. albicans* cause a pro-inflammatory immune response[56,65], these data support our notion that polymer LH can act on protein glycosylation.

The cell wall of *C. albicans* is adaptive and constantly remodels, including when *C. albicans'* transitions from yeast to hyphae, a process that is commonly associated with virulence[65]. Hence, we tested *C. albicans* under hypha-inducing conditions (37 °C and 5% CO_2) in the presence of antifungal polymers at sub-inhibitory concentrations over 4, 6 (to measure hypha length), and 24 h (to measure microcolony diameter) (Supplementary Fig. S24). Treatment with each polymer, especially LH, reduced the hyphal length and the diameter of microcolonies. Besides lytic activity against synthetic membranes isolated from *C. albicans* hyphae (see Fig. 3I, grey line), a reduced speed of hyphae formation could be beneficial for clearance and protection of epithelial cells, as the formation of hyphae drives cell invasion and infection of human epithelial cells by *C. albicans*[70], however, further studies are necessary to confirm this correlation for polymer LH.

Polymer LH prevents in vitro infection of human epithelial cells by *C. albicans* synergistically with caspofungin or fluconazole

During systemic infection, *C. albicans* hyphae invade the human epithelial barrier and allow it to spread *via* the bloodstream to distal organs[71]. The yeast-to-hypha transition is also important for common superficial infections, such as those of the vaginal mucosa, which affect approximately 75% of women worldwide at least once in their lifetime[72,73]. To investigate the therapeutic potential of polymer LH, we used an in vitro human epithelial cell model (HECM). Monolayers of vaginal epithelial cells (A-431) were infected with *C. albicans*, after the addition of different drug dilutions with minimum preincubation time. After 24 h, epithelial damage to A-431 cells was assayed by lactate dehydrogenase (LDH) release. Despite being a rather simple model, it has been routinely used to simulate vaginal candidiasis in vitro[74,75].

First, we examined the biocompatibility of polymer LH in the HECM in the absence of *C. albicans* (Supplementary Fig. S25, light-grey bars). Only at concentrations above 128 μg/mL (4–8× MIC against *C. albicans*) we observed more than 50% damage. Previously, polymer LH has similarly been reported to cause more than 50% damage against murine fibroblasts at 128 μg/mL or higher[27]. Based on the therapeutic index – the ratio of cytotoxic concentration to MIC – polymer LH, with its therapeutic index of 4–8, outperformed AmpB (therapeutic index 2–4)[27]. For the HECM in the present study, this would theoretically present a therapeutic window for polymer LH of up to 128 μg/mL. However, in the HECM at concentrations between 16 and 128 μg/mL, polymer LH did not prevent damage by *C. albicans* to the vaginal epithelial cells (Supplementary Fig. S25, dark-grey bars).

One possibility for the unexpected failure of LH to prevent damage in the HECM could be the bioavailability. To test this hypothesis, we pre-treated *C. albicans* cells with the polymer for 1 h at concentrations between 16 and 512 μg/mL before infection. Damage by *C. albicans* was strongly reduced with this altered protocol in a concentration-dependent manner up to 256 μg/mL (34% of untreated infection control at 256 μg/mL, Supplementary Fig. S26A). This supports the hypothesis that poor bioavailability in the HECM reduces the antifungal properties of the polymer. We next took supernatants from uninfected vaginal epithelial cells, treated with LH, and added them to *C. albicans* in a conventional MIC assay. These were unable to inhibit *C. albicans* growth in vitro, even when the initial concentration of polymer LH exceeded the MIC (Supplementary Fig. S26B). This suggests that the presence of human cells reduces the concentration of polymer in the supernatant. In contrast, the common antifungal drugs AmpB, caspofungin, and fluconazole (among others) successfully reduced damage by *C. albicans* to the epithelial cells in the HECM (Supplementary Table S2).

Since the polymer LH alone unexpectedly did not inhibit damage by *C. albicans* in the HECM, we studied combinations of LH with established antifungal compounds, first at MIC assay conditions and without human cells (Supplementary Figs. S27 and 28, and Table S3). Synergy was defined as a minimum two-fold decrease in MIC in the presence of the other drug (fractional inhibitory concentration (FIC) index ≤0.5). Antagonistic drug combinations result in an FIC index of at least 4, *i.e.*, a MIC increase of at least two-fold. Indifferent (FIC index = 1), and additive (FIC index between 0.5 and 1) effects were also considered.

The compounds selected for our synergy studies differ in their targets: cell wall (Calcofluor White, Congo Red, caspofungin, nikkomycin Z); cell membrane (AmpB, cetyltrimethylammonium bromide (CTAB), dodecyltrimethylammonium bromide (DTAB), sodium dodecyl sulfate (SDS)); or intracellular processes (fluconazole, cycloheximide, tunicamycin, FK506, geldanamycin), which in turn could again affect cell membrane or wall composition. Seven out of these thirteen antifungal compounds showed a synergistic or strong additive effect (FIC index below 0.6) with LH in vitro and were therefore tested in the HECM. In addition to the LDH release assay, propidium iodide was used to visualise dead epithelial cells after 24 h of infection (Fig. 5, Supplementary Fig. S29).

Although LH alone did not prevent damage by *C. albicans* (Supplementary Fig. S26), it did so in combination with the antifungal drugs caspofungin or fluconazole, even at normally sub-inhibitory

https://doi.org/10.1038/s41467-024-50491-x

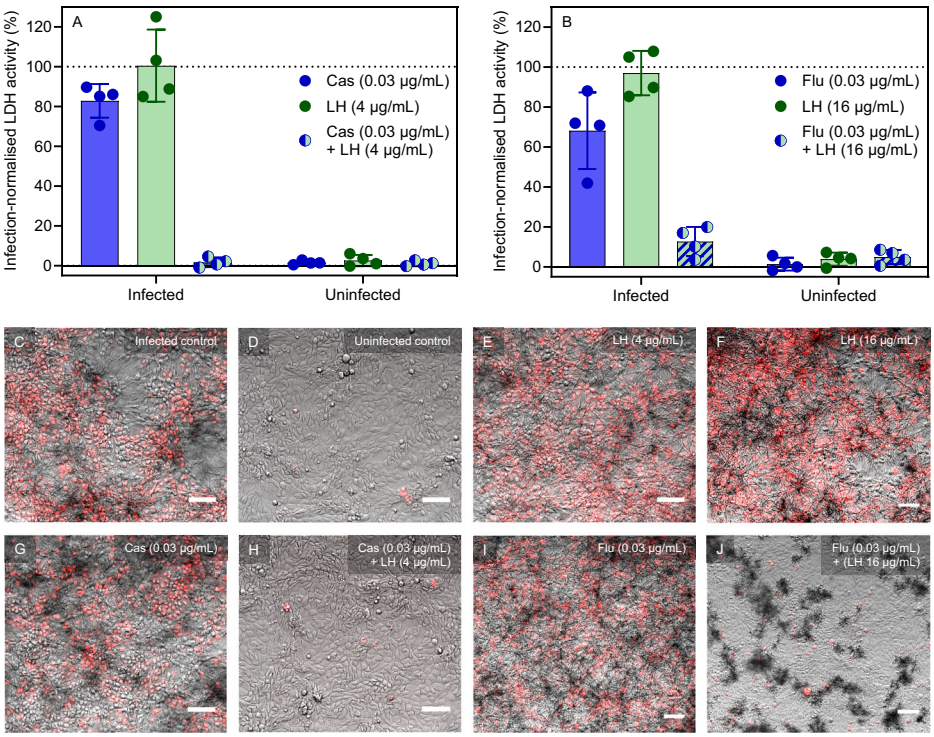

Fig. 5 | Synergistic effects of LH in combination with selected antifungal drugs against *C. albicans* SC5314 during vaginal epithelial cell infections. Damage to vaginal epithelial (A-431) cells (infected by *C. albicans* and uninfected) after treatment with polymer LH and **A** caspofungin (Cas) or **B** fluconazole (Flu) and their respective combinations was measured by LDH release ($n = 4$ biological replicates, SD around the mean). Damage to A-431 cells was normalised to untreated infection control (for infected samples) or a Triton-X-treated 100% lysis control (uninfected samples; each indicated by a dotted line). Source data are provided as a Source Data file. (**C**–**J**) show fluorescence microscopy images of the scenarios represented in (**A**) and (**B**) to visualise morphological changes and the viability of vaginal epithelial cells by staining with 1 μg/mL propidium iodide. Scale bars represent 100 μm.

concentrations (Fig. 5). Strikingly, only 0.03 μg/mL of caspofungin (*i.e.*, 8× less than its MIC of 0.25 μg/mL in the HECM) combined with 4 μg/mL LH was required to reduce host cell damage to 2% with no visible cytotoxicity (Fig. 5A). Similarly, a low dose of 0.03 μg/mL fluconazole (again 8× less than its MIC in the HECM) combined with 16 μg/mL LH reduced vaginal epithelial cell damage to 13%, while remaining biocompatible (Fig. 5B). Without LH, these low antifungal drug concentrations did not prevent infection with over 50% epithelial cell damage. This finding was supported by fluorescence microscopy (Fig. 5C–J), where the same combinations resulted in healthy vaginal epithelial cells and low doses of antifungal drugs did not significantly protect the epithelial cells from damage at up to 0.25 μg/mL. Combination with LH therefore reduced the MIC for established antifungal drugs up to eight-fold, showing its potential as a synergistic agent for antifungal applications.

The other antifungal compounds with strong additive or synergistic behaviour with LH in the in vitro pre-screen (nikkomycin Z, cycloheximide, tunicamycin, FK506, geldanamycin), did not reduce damage to epithelial cells to less than 45% of the no-drug control, and in some cases showed no significant synergism (Supplementary Fig. S29). Some of those compounds are cytotoxic at elevated concentrations, and indeed, the combination of LH with cycloheximide or geldanamycin caused damage to uninfected human cells.

Combination of polymer LH and caspofungin prolongs survival in an invertebrate model of *C. albicans* infection

Next, we assessed whether the synergism of polymer LH with caspofungin protected against fungal infection in vivo. For this, we used the well-established *Galleria mellonella* (greater wax moth) model of systemic candidiasis by injecting larvae with an infectious dose of *C. albicans* followed by treatment with LH and caspofungin[76–79]. Even though *G. mellonella* is an invertebrate organism, the model has several advantages for testing the virulence of *Candida* spp. and antifungal activity of candidate antifungals, such as ease-of-use, growth at 37 °C, and its many similarities to the mammalian innate immune system[76–79].

We first determined the acute toxicity of polymer LH, caspofungin, and AmpB in larvae. Lethal effects of LH on larvae were observed at 500 mg/kg or higher (Supplementary Fig. S30A). No toxicity was observed for caspofungin at doses up to 100 mg/kg (Supplementary Fig. S30B, blue line), AmpB showed toxicity at 100 mg/kg after 4 d (Supplementary Fig. S30B, purple line). Therefore, both LH and caspofungin outperformed AmpB in terms of toxicity, and we determined that doses of LH up to 250 mg/kg and caspofungin up to 100 mg/kg could be used to treat larvae. The synergistic combination of LH with fluconazole was not tested, because it was not active against *C. albicans* in the presence of 50% (v/v) or more of foetal bovine serum in MIC assays, in contrast to the combination of LH and caspofungin which remained active in the presence of serum (Supplementary Table S4).

To simulate systemic candidiasis, we infected each larva with 1×10^5 *C. albicans* cells in one proleg, treated them in another proleg, and monitored survival over 14 days (Fig. 6). All uninfected, water-treated *G. mellonella* larvae survived for 14 d. In contrast, untreated and water-mock treated *C. albicans*-infected larvae died after 2 d (difference not significant at $p = 0.674$).

Treatment with 100 mg/kg caspofungin alone protected 94.7% of the larvae from death, whereas only 10.5% of larvae survived to 14 d at 5 mg/kg (Fig. 6). All infected larvae treated with polymer LH alone at 250 mg/kg succumbed by day 3, however, the same dose in

https://doi.org/10.1038/s41467-024-50491-x

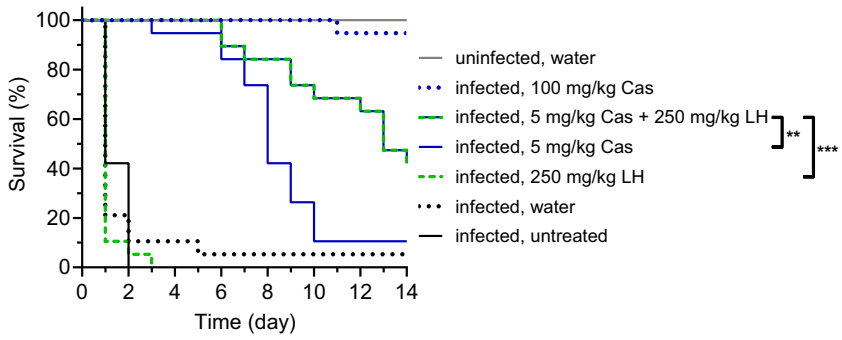

Fig. 6 | Treatment with polymer LH in combination with caspofungin (Cas) prolongs survival of *C. albicans*-infected *Galleria mellonella* larvae. *G. mellonella* larvae were infected with 1×10^5 *C. albicans* cells (except uninfected control, grey) and treated after 2 h with caspofungin (Cas; 5 mg/kg: blue; 100 mg/kg: blue dotted), polymer LH (250 mg/kg, green dashed), and the combination of 5 mg/kg Cas and 250 mg/kg LH (green and blue dashed). Untreated, infection controls are shown in black (*C. albicans* only) or black dashed (*C. albicans*, injected with water). Survival of *G. mellonella* was monitored over 14 d. Nineteen larvae per condition were tested. Statistical significance was determined for infected larvae treated with the combination (5 mg/kg Cas + 250 mg/kg LH) compared to infected larvae treated with the respective dose of a single drug by Log Rank (Mantel–Cox) pairwise comparison (**$p < 0.01$ [here: $p = 0.003$], ***$p < 0.001$). At the concentrations used here, the single compounds exhibited no toxicity against *G. mellonella*, as shown in Supplementary Fig. S30. Source data are provided as a Source Data file.

combination with low-dose caspofungin (5 mg/kg) significantly increased the survival of *C. albicans*-infected larvae (5 mg/kg caspofungin vs. combination: $p = 0.003$; 250 mg/kg LH vs. combination: $p < 0.001$; water vs. combination: $p < 0.001$). Compared to low-dose caspofungin treatment, the survival after 14 d increased four-fold to 42.1%. Notably, 100% of infected larvae treated with the synergistic combination survived until day 6 post-infection. This therefore demonstrates in vivo synergy between polymer LH and caspofungin and emphasises the in vivo potential of the synthetic polymer LH in combination therapy. Such combination therapy approaches of compounds which are individually inactive or only marginally active in vivo have received more attention recently. Examples include an AFP mimic (brilacidin) potentiating caspofungin and a small organic molecule (imidazopyrazoindole) synergising with azoles[17,18]. Notably, the possibility of re-sensitising drug-resistant fungi by the combination of active compounds is promising[17,18,20]. The key advantages of synthetic polymers are stability and cost-effective production at scale[20,30], which could solve many issues, especially in low-income countries[9].

In vitro evolution leads to tolerance of *C. albicans* to LH, but not to the combinations of LH with caspofungin or fluconazole

A major obstacle in the development of antifungal drugs is the emergence of resistance. In this study, we follow the definition of resistance and tolerance suggested by Berman and Krysan[80]; where resistance is the clinically observed ineffectiveness of a drug against a fungal pathogen and tolerance is the slow growth of a less susceptible fungal strain at normally inhibitory concentrations in vitro[80]. An in vitro evolution assay (Fig. 7A) was used to determine whether prolonged exposure to polymer LH, caspofungin, fluconazole or their synergistic combinations results in the emergence of tolerant *C. albicans* variants. Growth at 1× MIC over 14 d (Fig. 7B) showed an increasing tolerance for the single drug treatments after 9–10 d incubation. A less pronounced tolerance developed for the combination of fluconazole and LH, while essentially no change in growth was seen for the combination of caspofungin and LH.

After 14 d, an aliquot of the cells was incubated at 2× MIC for 24–48 h. If growth was observed, the sample was plated, single colonies were isolated and their MIC to the antifungal polymers (LP, LH, CB, and CX) and antifungal drugs (AmpB, fluconazole, caspofungin, tunicamycin) was determined (Supplementary Table S5). Isolates with an increased MIC were selected for further analysis (Fig. 7B, filled circles – increased tolerance to LH, empty circles – no increase in LH tolerance). In agreement with their growth pattern over 14 d, we did not find any stably tolerant isolates after treatment with combinations of LH and caspofungin or fluconazole (MICs in Supplementary Table S5).

To identify the genetic basis for LH tolerance, we sequenced the genomes of three independent LH-evolved strains with high MIC (evo-LH1, evo-LH2, and evo-LH3, filled black circles in Fig. 7B), and a fluconazole-evolved strain (evo-Flu1) as control. Evo-LH1 showed an increase in MIC against LH to 64–128 μg/mL and was also more tolerant to the polymers LP, CB, and CX. The MICs towards established antifungal drugs (AmpB, caspofungin, fluconazole, tunicamycin) remained unchanged. Interestingly, evo-Flu1 not only showed increased tolerance to fluconazole (MIC 2 μg/mL) but also to caspofungin and the polymers. The caspofungin-evolved strain (evo-Cas1) developed an increased MIC for caspofungin (2 μg/mL), but we did not observe any cross-tolerance.

To investigate the genomic mechanisms of *C. albicans* adaption to LH or fluconazole, we examined the gene counts for the evolved strains compared to wild-type *C. albicans* SC5314 (Fig. 7C, Supplementary Fig. S31). In all strains, including the parental wild-type SC5314, loss of heterozygosity was detected in the left arm of chromosome 2 (Supplementary Fig. S31). Analysis of the evolved strains revealed major ploidy changes in some cases: In evo-Flu1, we observed aneuploidy of chromosome R and trisomy of chromosome 5. Both are associated with fluconazole resistance[81,82], and the chromosome 5 trisomy has been shown to be driven by amplification of the *ERG11* and *TAC1* genes[83]. For evo-LH1 and evo-LH2, we found aneuploidy in chromosome R, and trisomy in chromosome 2, respectively. Notably, chromosome 2 trisomy and tetrasomy have been linked to adaption to the ER stressor tunicamycin[84]. For the strain evo-LH3, which showed only a minor change in MIC, we found no large-scale ploidy changes.

We did not find mutations or copy number variations on the gene level that could explain the drug tolerance phenotype, although some differences were observed between our isolated *C. albicans* strains on the nucleotide level (Supplementary Data S2). We conclude that major chromosomal aberrations probably drive tolerance to polymer LH in *C. albicans*. Together with our transcriptomics and chemical-genetic screening evidence, we therefore postulate that polymer LH has multiple targets, which differ from those of known antifungal drugs.

Importantly, in our in vitro evolution experiment we found no development of genetically stable tolerance by combinatorial treatment of LH with caspofungin or fluconazole, in further support of our hypothesis of distinct targets. The strong synergistic action with caspofungin against *C. albicans* on human epithelial cells in vitro and *G. mellonella* larvae in vivo, together with the reduced tolerance

https://doi.org/10.1038/s41467-024-50491-x

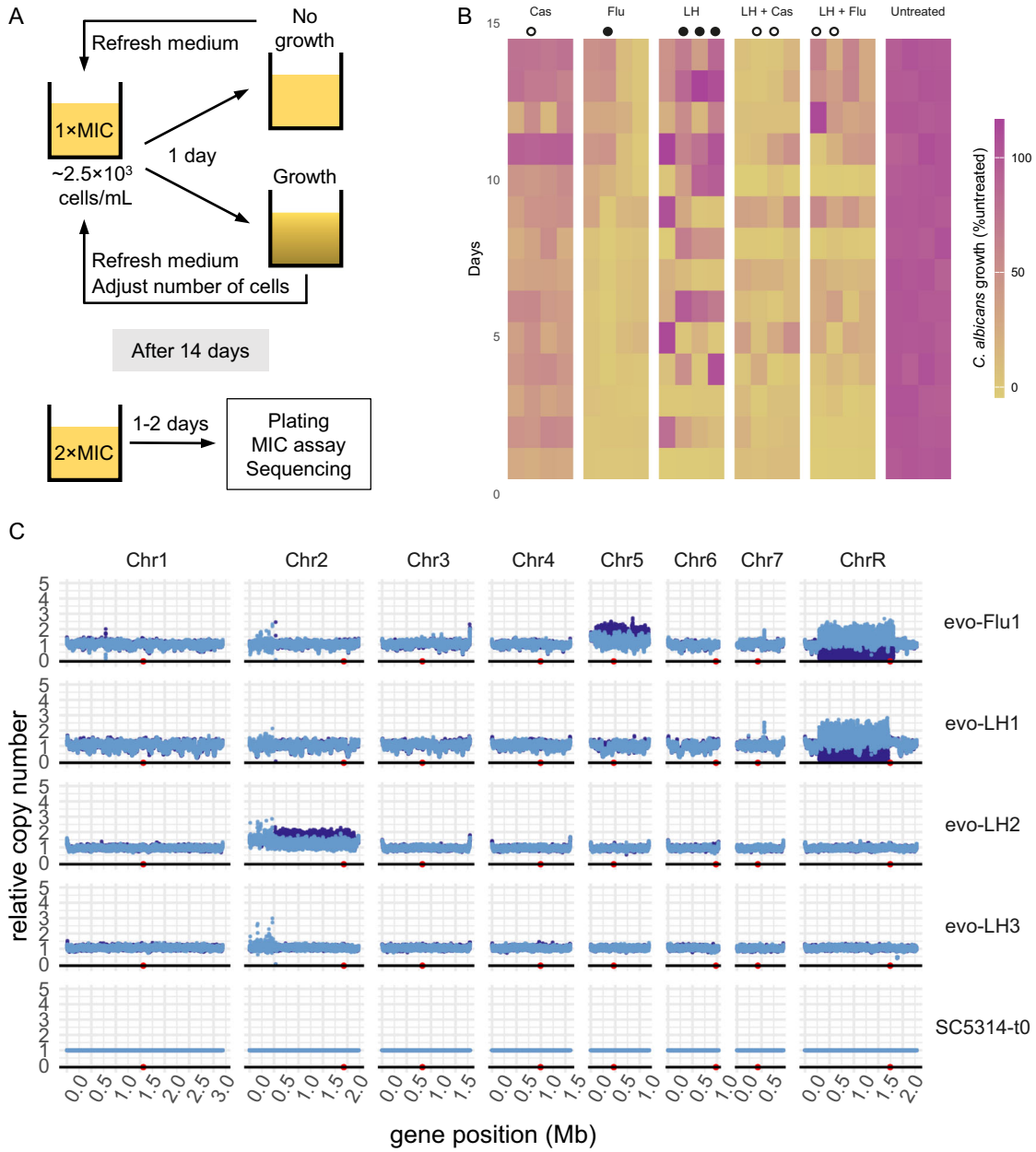

Fig. 7 | In vitro evolution experiment of *C. albicans* challenged with 1× MIC of caspofungin (Cas), fluconazole (Flu), polymer LH, and the synergistic combinations. A Experimental setup of the in vitro evolution experiment. **B** Growth of *C. albicans* was monitored by absorbance over 14 d and normalised to the untreated controls. Filled circles highlight strains that were selected for whole genome sequencing and empty circles highlight strains additionally analysed for their MIC against antifungal compounds in Supplementary Table S5. Source data are provided as a Source Data file. **C** Genomes of the isolated strains with the highest tolerance to antifungal drugs were sequenced and analysed for their relative copy number for Flu- and LH-evolved strains. Each point in (**C**) represents the mean normalised read depth compared to wild-type *C. albicans* strain SC5314 at $t = 0$ for a gene (Y-axis) on its chromosome position (X-axis), colour-coded by allele. Positions of the centromeres are indicated by red circles. The MICs for Flu and LH are indicated on the right, where MIC in SC5314 is depicted in green and higher values scale to red.

development suggests that the amphiphilic polymer LH is a promising antifungal lead for combination therapy with well-established drugs.

In summary, we investigated four synthetic polymers, which were inspired by amphiphilic antimicrobial peptides and which kill drug-resistant clinical *C. albicans* isolates. Our findings reveal that the most promising polymer, LH, exerts its activity on *C. albicans* by a putatively novel mode of action. We found evidence that it targets protein glycosylation, and also interferes with the fungal membrane, which together leads to fungal cell death. The combination of LH with caspofungin is particularly promising in its therapeutic potential since it inhibits infection of human epithelial cells by *C. albicans* at otherwise sub-inhibitory concentrations and additionally increases fungal uptake by human macrophages. Moreover, the synergistic combination of polymer LH and caspofungin prolonged survival in an in vivo model of systemic candidiasis. In addition to these promising synergistic effects, which prevent *C. albicans* infection in vitro and protect in vivo, the combination of polymer LH and caspofungin did not lead to any tolerant *C. albicans* strains after prolonged exposure in vitro, highlighting the therapeutic potential of polymer LH as an antifungal lead, particularly for combination therapy. Future experiments may allow to further optimise polymer LH, *e.g.*, by investigating the effect of monomer sequence or block order within the polymer on its activity.

This way, it may be possible to retain the promising antifungal activity even as a stand-alone formulation, which would then also be envisioned to be tested in vertebrate in vivo infection models.

Methods

Ethics statement

The research presented here complies with all relevant ethical regulations. The blood donation procedure was approved by the Jena institutional ethics committee (Ethik-Kommission des Universitätsklinikums Jena, Permission No 2207–01/08). All donors gave written informed consent and did not receive any compensation. Age, sex or gender of the donors was not taken into account.

Materials for polymer synthesis

Ethylenediamine (Sigma-Aldrich, ≥99%), *N*-amylamine (Sigma-Aldrich, 99%), *N*-benzylamine (Sigma-Aldrich, 99%), *N*-heptylamine (Sigma-Aldrich, 99%), *N*-cyclohexanemethylamine (Sigma-Aldrich, 98%), di-tert-butyl dicarbonate (Sigma-Aldrich, 99%), *N*-hydroxyethyl acrylamide (Sigma-Aldrich, 97%), triethylamine (TEA) (Scharlau, 99%), trifluoroacetic acid (TFA) (Sigma-Aldrich, 99%), chloroform (Merck), dichloromethane (DCM) (Merck), tetrahydrofuran (THF) (Merck), diethyl ether (Merck), hexane (Merck), dimethyl sulfoxide (DMSO) (Merck), dimethylacetamide (DMAc) (Sigma-Aldrich), thionyl chloride (Sigma-Aldrich, 99%), acrylic acid (Sigma-Aldrich), deuterated DMSO (Cambridge Isotope Laboratories, Inc.), 2-(butylthiocarbonothioylthio) propanoic acid (BTPA, Boron Molecular) and 5,10,15,20-tetraphenyl-21*H*,23*H*-porphine zinc (ZnTPP) (Sigma-Aldrich) were used as received.

Acryloyl chloride synthesis

Acryloyl chloride was synthesised according to the previously reported procedure[85], with slight changes[27]. Briefly, acrylic acid (41.2 mL, 1.2 equiv) was added dropwise to 36.3 mL of thionyl chloride at 0 °C over 45 min under nitrogen. The mixture was stirred for 12 h at 40 °C. The product was collected by in situ distillation under atmospheric pressure.

Synthesis of monomers

Cationic monomer - tert-butyl (2-acrylamidoethyl)carbamate. *tert*-Butyl (2-acrylamidoethyl)carbamate was prepared according to the previously reported procedure[27,86,87] Ethylenediamine (0.33 mol) was dissolved in chloroform (400 mL). Di-*tert*-butyl dicarbonate (0.03 mol) was dissolved in 100 mL of chloroform and was added dropwise to the ethylenediamine solution over 4 h at 0 °C while stirring and continued overnight at room temperature. After filtering the white precipitate, the organic phase was washed with 200 mL of Milli-Q water six times and then dried using $MgSO_4$. Solids were separated by filtration, and chloroform was evaporated, resulting in a pale yellow oil. THF (100 mL) was added to dissolve the obtained oil. TEA (1.2 equiv) and acryloyl chloride (1.1 equiv) were added dropwise to the solution at 0 °C with N_2 bubbling. The reaction mixture was stirred at room temperature for 2 h. Afterwards, THF was removed by rotary evaporation. The crude product was dissolved in chloroform (150 mL) and washed with 0.1 M HCl solution (1 × 75 mL), saturated $NaHCO_3$ (1 × 75 mL), brine (1 × 75 mL), and water (1 × 75 mL). The organic phase was dried using $MgSO_4$ and filtered, and the remaining solvent was removed by rotary evaporation. The product was further purified by repeated precipitation steps in hexane to yield the Boc-protected monomer as a fine white powder, which was dried *in vacuo*.

Synthesis of hydrophobic monomers. A standard procedure, as previously reported[27,87] was employed for the synthesis of four hydrophobic monomers ((*N*-pentylacrylamide, *N*-heptylacrylamide, *N*-cyclohexanemethyl)acrylamide, and *N*-benzylacrylamide) from their corresponding amines (*N*-amylamine, *N*-heptylamine, *N*-cyclohexanemethylamine, or *N*-benzylamine) using acryloyl chloride: The specified amount of amine was dissolved in THF with a ratio of 6 mL of THF per 1 mmol amine. TEA (1.2 equiv) and acryloyl chloride (1.2 equiv) were added in a dropwise manner at 0 °C with N_2 bubbling and further stirred overnight at room temperature. The by-products were filtered, and the solvent was removed by rotary evaporation. The crude product was dissolved in chloroform (1.5× THF volume), washed sequentially with 0.1 M HCl, saturated $NaHCO_3$, brine, and water using half of the chloroform volume for each wash. The organic phase was dried with MgSO4 and basic Al2O3 and filtered to remove solids. Finally, the solvent was removed by rotary evaporation and dried in vacuo to yield the acrylamide monomer.

Random copolymerisation by photo-induced electron/energy transfer-reversible addition-fragmentation chain transfer (PET-RAFT) polymerisation

The linear, random copolymers were synthesised using a slight modification of the general one-pot protocol reported previously[88] Briefly, stock solutions of the monomers were prepared with a concentration of 33% (w/w) in DMSO. ZnTPP was dissolved in DMSO at a concentration of 1 mg/mL. The RAFT agent BTPA was added to a 4 mL glass vial in an amount corresponding to the targeted X_n of 20 and dissolved in DMSO. Monomer stock solutions were added into the vial to a final monomer concentration of 25% (w/w) in DMSO, corresponding to the targeted ratios. The photocatalyst (ZnTPP) was added at 100 ppm relative to the monomers. The vial was sealed with a rubber septum, and the headspace was degassed with N_2 for 10 min. The vial was then placed under a green light-emitting diode light (λ = 530 nm) for 20 h to produce the Boc-protected copolymers. The copolymers were analysed by size-exclusion chromatography (SEC) and ^{1}H nuclear magnetic resonance (NMR) to examine the monomer conversion, polymer composition, and molecular weight distribution. Then, the polymer was purified by precipitating in a diethyl ether/hexane mixture (3:7), followed by centrifugation (5000 × *g* for 5 min, 0 °C). The precipitate was dissolved in acetone or methanol and reprecipitated twice more. The polymer was then dried *in vacuo* prior to Boc-group removal.

Polymer deprotection. TFA was used to remove Boc-protecting groups based on our group's previously reported protocol[88] Briefly, the polymer was dissolved in DCM (~7% (w/w) polymer), followed by the addition of TFA (20 mol equivalent with respect to Boc groups). The mixture was stirred at room temperature for 3 h and precipitated into diethyl ether. The precipitate was isolated by centrifugation, dissolved in acetone, and reprecipitated twice more. The polymer was then dried *in vacuo*, and ^{1}H NMR analysis was used to determine the removal of Boc-protective groups and to examine the targeted X_n.

Polymer characterisation. ^{1}H NMR spectra were obtained using a Bruker AVANCE III spectrometer (300 MHz, 5 mm BBFO probe) or a Bruker AVANCE III 400 spectrometer (400 MHz, 5 mm BBFO probe). Deuterated DMSO was used as a solvent to determine the polymer composition and conversion at concentrations of ~10–20 mg/mL. All experiments were run with a gas flow across the probes at 535 L/h with sample spinning and at a temperature of 25 °C. All chemical shifts were stated in parts per million (ppm) relative to tetramethylsilane.

SEC analysis was performed using a Shimadzu liquid chromatography system equipped with a Shimadzu refractive index detector and three MIX C columns operating at 50 °C. DMAc (containing 0.03% (w/v) LiBr and 0.05% (w/v) 2,6-dibutyl-4-methylphenol) was used as the eluent at a flow rate of 1 mL/min. The system was calibrated using narrow poly(methyl methacrylate) (PMMA) standards with molecular weights from 200 to 10^6 g/mol.

Media and buffers for biological experiments

Phosphate-buffered saline (pH 7.4). A 10× phosphate-buffered saline (PBS) stock (1.37 mol/L sodium chloride, 0.027 mol/L potassium

Table 3 | Concentrations, medium and storage temperature of antifungal stocks

Antifungal compound	Stock concentration		Medium	Storage temperature
	mg/mL	mM		
Amphotericin B (AmpB)	1–2	1.1–2.2	DMSO	4 °C
Calcofluor white	50	5.5	DMSO	−20 °C
Caspofungin	1	0.9	Distilled water	−20 °C
Cetyltrimethylammonium bromide (CTAB)	10	27.4	Distilled water	Room temperature
Congo red	6	8.6	Distilled water	4 °C
Cycloheximide	5	17.8	Distilled water	4 °C
Dodecyltrimethylammonium bromide (DTAB)	10	32.4	Distilled water	Room temperature
FK506	5	6.2	DMSO	−20 °C
Fluconazole	1–2	3.3–6.5	DMSO	4 °C
Geldanamycin	5	8.9	DMSO	−20 °C
LL-37	1	0.2	Distilled water	−20 °C
Nikkomycin Z	5	10.1	Distilled water	4 °C
Sodium dodecyl sulfate (SDS)	10	34.7	Distilled water	Room temperature
Tunicamycin	5	5.9	DMSO	4 °C

chloride, 0.08 mol/L disodium hydrogen phosphate, 0.02 mol/L potassium dihydrogen phosphate) was prepared by dissolving 80.06 g sodium chloride, 2.01 g potassium chloride, 11.36 g disodium hydrogen phosphate, and 2.72 g potassium dihydrogen phosphate in 900 mL of double-distilled water and the pH was adjusted to 7.4, before adding double-distilled water up to a final volume of 1 L. The solution was autoclaved for sterilisation. A 1× PBS solution was obtained by dissolving 100 mL of 10× PBS in 900 mL of sterile double-distilled water.

Yeast extract peptone dextrose medium. The yeast extract peptone dextrose (YEPD; 1% (w/v) yeast extract, 2% (w/v) mycological peptone, and 2% (w/v) D-glucose) broth was prepared by dissolving 4 g yeast extract and 8 g mycological peptone in double-distilled water up to a total volume of 360 mL. After autoclaving, 40 mL of filter-sterilised 20% (w/v) D-glucose was added. For YEPD plates, 8 g agar was added to the solution before autoclaving.

Synthetic defined medium. Synthetic defined (SD) medium was prepared by dissolving 6.7 g yeast nitrogen base (YNB) without amino acids, and 0.395 g complete supplement mixture were dissolved in 900 mL double-distilled water, adjusted pH to 6.0 with HCl and NaOH, and autoclaved. Afterwards, 100 mL of filter-sterilised 20% (w/v) D-glucose was added. When required, 5 mL of a filter-sterilised 5 mg/mL uridine solution was added, too.

Modified Roswell Park Memorial Institute (RPMI)-1640 medium for *C. albicans* studies. To 1 L of RPMI-1640 medium (with L-glutamine, without bicarbonate), 18 g D-glucose and 34.53 g 3-(*N*-morpholino) propane-1-sulfonic acid (MOPS) were added. Afterwards, the pH was adjusted with HCl and NaOH to 4.0 and filter-sterilised.

Polymer and antifungal stock solutions

Polymer stock solutions were prepared at a concentration of 10 mg/mL (3.4–3.7 mM, depending on the respective polymer composition) in sterile distilled water and stored at 4 °C. Before use, the stock solutions were sonicated for approx. 3 min.

Antifungal drug stocks were prepared at different stock solutions in sterile distilled water or DMSO, as summarised in Table 3.

Culture conditions of fungal strains

The yeasts were routinely streaked on YEPD agar and incubated for 1–2 days at 30 °C (37 °C for clinical isolates). Cultures on agar plates were stored for up to two weeks at 4 °C. Long-term stocks were stored at −80 °C in 50% (v/v) sterile glycerol from an overnight culture. Overnight cultures were prepared by inoculating colonies from a YEPD plate in YEPD broth and shaking overnight at 30 °C at 180 rpm (37 °C for clinical isolates).

Fungal strains

A complete list of used fungal strains is attached in Supplementary Data S3. For most assays, the *C. albicans* reference strain SC5314 was used, unless otherwise indicated.

Minimum inhibitory concentration (MIC) assay and evaluation of drug interactions

The MICs of polymers against different strains of *C. albicans* were determined *via* the broth microdilution method according to Clinical and Laboratory Standards Institute (CLSI) guidelines for fungal susceptibility testing, with slight modifications[32,33]. Briefly, the *C. albicans* strains were grown on YEPD plates for 48 h at 30 °C (37 °C for clinical isolates). One colony was emulsified in 1 mL of sterile Milli-Q water. Cells were counted using a haemocytometer and adjusted to $2–5 \times 10^6$ cells/mL. The cell suspension was diluted 1:1000 in the modified RPMI-1640 medium (supplemented with D-glucose and MOPS, pH 4.0) to obtain the 2× concentrated stock suspension. A two-fold dilution series of the 100 µL polymer solution was added into 96-well microplates (final concentration between 4 and 512 µg/mL), followed by the addition of 100 µL of fungal cell suspension. The 96-well plates were incubated for 24 h at 35 °C in a humidified chamber, wells were resuspended, and the absorbance was measured at 405 nm with a microtiter plate reader. Additionally, AmpB, fluconazole, and caspofungin were tested at final concentrations between 0.125 and 16 (AmpB) and 0.06–8 µg/mL (fluconazole and caspofungin). DMSO controls at the respectively used final concentrations, no-polymer and no-cell controls were included in all experiments. The MIC value was defined as the lowest concentration of the respective polymer that showed growth inhibition of >90% compared to the untreated control. Three independent biological replicates were carried out (unless otherwise indicated).

To evaluate interactions of the polymer LH with selected antifungal compounds (see Table 3), C. *albicans* cells were treated and prepared as described above. The drug-dilution plates were prepared separately for each drug before combining them. For that, a four-fold dilution series of the respective antifungal drug was added into a 96-well microplate along the rows. The same was performed with polymer

LH, diluting it in a 96-well microplate along the columns. Then, 50 μL of antifungal were combined with 50 μL of polymer LH, resulting in a two-fold dilution series of the respective compounds. Thereby, one row and one column acted as controls only containing one compound. Drug interactions were classified according to their fractional inhibitory concentration (FIC) indices. The FIC index was calculated as described in the following Eq. (1), where $c_{A/B}$ are the concentrations of compounds A or B, respectively, in combination resulting in growth inhibition >90%, and MIC_A and MIC_B are the MICs of compound A or B, respectively, alone:

$$\text{FIC index} = \frac{c_A}{MIC_A} + \frac{c_B}{MIC_B} \quad (1)$$

A combination was called synergistic if the FIC index was below 0.5, antagonistic for an FIC index above 4 and values in between as additive (between 0.5 and 1.0) or indifferent (between 1 and 4). Three independent biological replicates were carried out.

The MICs of polymer LH against *C. albicans* SC5314 in all used media are displayed in Supplementary Table S6.

RNA isolation, microarray and KEGG pathway/GO term enrichment analysis

For RNA isolation, *C. albicans* SC5314 was grown in YEPD broth overnight, diluted 1:50 in YEPD broth and subcultured for 4 h (30 °C, 180 rpm). The cells were washed three times in PBS (2500 × *g*, 1 min) and adjusted to approx. 5×10^7 cells/mL in SD broth. The cell suspension was added to a final concentration of approx. 5×10^6 cells/mL into sterile glass flasks containing 6 mL SD medium supplemented with no polymer (for the untreated control) or 32 (LH, LL-37), 64 (CB and CX), or 128 μg/mL (LP and poly-HEA) polymer, corresponding to their MICs (Table 2) and being sub-inhibitory at the conditions of this assay (Supplementary Table S6). The flasks were incubated for 1 h at 30 °C and 180 rpm. Three biological replicates were performed for each condition. Cell viability was ascertained by backplating on YEPD agar. Fungal cells were harvested for subsequent RNA isolation (2500 × *g*, 2 min, 4 °C) and handled on ice from that step onwards. RNA was then isolated using an RNeasy mini kit (QIAGEN) by mechanical disruption with acid-washed glass beads following instructions in the manual. The concentration and quality of RNA were checked by Nanodrop ND-1000 (ThermoScientific) and Bioanalyzer 2100 (Agilent). The Quick Amp Gene Expression Labeling Kit (Agilent) was used to synthesise Cy5-labelled cRNA. A common reference (RNA from a mid-log-phase-grown *C. albicans* SC5314[89]) was labelled with Cy3 following the same procedure. The dye incorporation was assured by spectrophotometric measurement using a NanoDrop ND-1000. Samples and common references were cohybridised on Agilent arrays (AMADID 026869) containing 15,744 *Candida albicans* probes corresponding to 6105 genes. The arrays were then scanned in a GenePix 4000B (Molecular Devices) with GenePix Pro 6.1 (AutoPMT; pixel size of 5 μm) and analysed with GeneSpring 14.8 (Agilent).

Data was log2-transformed and normalised to untreated wild-type SC5314. A heatmap with dendrogram depicting hierarchal clustering (based on Euclidean distance) was generated with base R (v4.3.2). PCA and k-means clustering ($K = 3$) was performed and plotted on R using packages stats and factoextra (v1.0.7). We performed KEGG pathway enrichment analysis on 0.5× up- or downregulated genes using clusterProfiler package (v4.10.1) on R[90,91]. For the gene set enrichment analysis, the parameters used were: minimum gene set size of 10, adjusted *p*-value of 0.05. For GO term enrichment analysis on at least 0.5× differentially regulated genes, the GO term finder online tool[45] on *Candida* Genome Database was used and assessed on 18/01/2023 with the following parameters: species and background set – *Candida albicans*; ontology – molecular function; adjusted maximum *p*-value of 0.1.

Mutant screening

A complete list of the tested mutants and reference strains is shown in the supplementary information (Supplementary Data S3). The experiments were generally performed in SD broth, supplemented with uridine if necessary.

Yeast cultures of the mutants were grown overnight at 30 °C, 180 rpm. The cultures were washed twice in PBS (1 min, 5000 × *g*). After counting with a haemocytometer, cell concentration was adjusted to approx. 10^6 cells/mL in SD broth and diluted 1:10. In a 96-well plate, 100 μL of yeast suspension was mixed with 100 μL of SD broth (untreated control) or SD broth supplemented with 2× concentrated antifungal polymers to reach final concentrations of 16 (LH), 32 (CB and CX), or 64 μg/mL (LP), corresponding to 0.5× MIC at the assay conditions (Supplementary Table S6). Reference strains relevant for the tested mutants were incubated with and without treatment alongside. All samples were prepared in technical duplicates and performed independently in triplicates. The 96-well plate was covered with sterile sealing foil. Growth curves were recorded with the infinite 200 or infinite 200Pro microplate reader (Tecan, i-control software) over 3 days at 30 °C by measuring absorbance at 600 nm every 15 min after orbital shaking for 10 s. To compare the growth curves of various mutants to their reference strains, a growth speed index based on time until half-maximum growth was used. The growth speed index was calculated as follows:

$$\text{Growth speed index} = -\log\left(\frac{M(\text{treated}) - M(\text{untreated})}{WT(\text{treated}) - WT(\text{untreated})}\right) \quad (2)$$

Here, *M* is time until half-maximum growth was reached for mutants, treated or untreated, and equally WT corresponds to the respective wild-type or reference strain. Thus, negative values display reduced growth speed in the presence of polymer and positive values reflect beneficial growth of the mutant compared to the reference strain in the presence of polymer.

Two- or four-fold increase of antifungal polymers consistently led to no growth of the yeast. In case of unexpected fast growth or late-onset growth at those elevated concentrations, the experiment was excluded and repeated.

Cell lysis assay *via* fluorescence microscopy

A *C. albicans* SC5314 mutant, expressing GFP intracellularly under the regulation of the constitutive *ADH1* promoter (*adh1*::P_{ADH1}-GFP CaSAT1) was grown overnight in YEPD broth. The cells were subcultured 1:50 in YEPD broth for 4 h (30 °C, 180 rpm), washed three times in PBS (2500 × *g*, 1 min) and diluted to 2×10^5/mL in modified RPMI (with glucose and MOPS, pH 4.0). Of this, 100 μL were added to 100 μL of 2× concentrated antifungal stock solutions in modified RPMI in technical duplicates in a 96-well plate to final concentrations of 16, 32, and 64 μg/mL polymer LH (0.25×, 0.5×, and 1× MIC at the conditions of this assay, Supplementary Table S6), 2 μg/mL AmpB (1× MIC), or 8 μg/mL tunicamycin (1× MIC) with a medium-only control. Inoculation counts were checked by backplating on YEPD. After 6 h incubation at 35 °C in a humidified chamber, samples from each well were backplated in duplicates on YEPD to check viability compared to the inoculum control and final cell counts. The 96-well plate was then centrifuged at 250 × *g* for 10 min, the supernatant removed carefully, and cells were fixed in 75 μL ROTI®Histofix (Carl Roth, Germany) for 30 min at room temperature. The plates were centrifuged again, supernatants discarded and 200 μL PBS added for microscopical analysis. A ZEISS Celldiscoverer 7 (20× plan-apochromat objective, 2× magnification, equipped with an Axiocam 506) was used for acquiring brightfield images (5–20 ms exposure) and detection of fluorescence (LED excitation at 470 nm for 500 ms, 501–547 nm emission filter). The ZEN software (blue edition, ZEISS) was used to normalise fluorescence of treated samples to untreated control.

Fluorescence intensities were quantified by region-of-interest measurements in ImageJ (v1.51)[92] of >50 *C. albicans* cells relative to untreated cells (100%). The experiment was repeated three times independently.

Lipid purification for synthetic membrane lysis

A *C. albicans* overnight culture (YEPD broth, 30 °C, 180 rpm) was diluted 1:50 in YEPD (for yeast cells) and RPMI-1640 (for hyphae). Subcultures were incubated for 3 h at 30 °C in glass flasks (yeast) or 37 °C and 5% CO_2 in stationary petri dishes (hyphae). Total lipids were prepared as described for extraction from *Saccharomyces cerevisiae* cells in ref. 93, with the following modifications: isolated *C. albicans* yeast or hyphae cells were resuspended in 15 mL 50% (v/v) methanol using an ultrasonication bath and disrupted at 40 kpsi using a One Shot Cell Disrupter (Constant Systems Ltd., UK). The flow path was flushed once with 15 mL 50% (v/v) methanol and the emulsion centrifuged. The pelleted debris was resuspended in 15 mL 150 mM ammonium bicarbonate and after the addition of 75 mL of chloroform:methanol (17:1), stirred for 60 min. The addition of 37 mL methanol led to a final chloroform:methanol ratio of 2:1, followed by further stirring for 60 min. The chloroform phase was collected using a separatory funnel and dried under reduced pressure using a rotary evaporator. After the addition of water, the extracted material was lyophilised.

Human erythrocytes were isolated by density centrifugation (Biocoll), washed three times with 45 mL 0.89% NaCl, and lipids extracted as described in ref. 94 by sequential addition of isopropanol (330 mL, 60 min) and chloroform (210 mL, 60 min). After sedimentation of haemoglobin by centrifugation, the dried supernatant was redissolved in chloroform:methanol (2:1, 10 mL) and threefold extraction with chloroform:methanol in a separatory funnel yielded the lipid extract. The lipid extract was dried by rotary evaporation, 2 mL chloroform and a small amount of water were added, the chloroform evaporated and the sample lyophilised.

Determination of membrane permeabilisation

Tethered membranes with 10% tethering lipids and 90% spacer lipids (T10 slides) were formed using the solvent exchange technique according to the manufacturer's instructions (SDx Tethered Membranes Pty Ltd). Briefly, 8 μL of 3 mM lipids solution in ethanol was added, incubated for 2 min and then 93.4 μL RPMI buffer was added. After rinsing 3× with 100 μL buffer the conductance and capacitance were measured for 20 min before injection of polymer LH, poly-HEA, or the antimicrobial peptide LL-37 at different concentrations. The substances were added sequentially so that the following concentrations were achieved in the measured volume. Concentrations of the two polymers were the same (20 min: 8 μg/mL, 50 min: 24 μg/mL, 80 min: 56 μg/mL, 110 min: 120 μg/mL, 140 min: 248 μg/mL), and of LL-37 they were 15× lower (20 min: 0.1 μg/mL, 50 min: 0.6 μg/mL, 80 min: 1.6 μg/mL, 110 min: 6.6 μg/mL, 140 min: 16.6 μg/mL). All experiments were performed at 37 °C and repeated three times in independent experiments. Signals were measured using the TethaPod (SDx Tethered Membranes Pty Ltd).

Transmission electron microscopy of *C. albicans*' cell wall

For transmission electron microscopy (TEM), a *C. albicans* overnight culture (YEPD broth, 30 °C, 180 rpm) was diluted 1:50 in YEPD and incubated for 4 h at 30 °C and 180 rpm. After centrifugation (2000 × *g*, 1 min), the pellet was washed in PBS and the cell concentration was adjusted to 10^7/mL in SD broth. Of this, 200 μL were added to 9.8 mL SD broth (untreated control), SD broth plus LH (128 μg/mL final concentration), SD broth plus tunicamycin (4 μg/mL), or SD broth plus poly-HEA (128 μg/mL) and incubated in glass flasks for 6 h at 180 rpm and 30 °C. Cell viability was checked by backplating on YEPD. The samples were centrifuged for 5 min at 4 °C and 1000 × *g*, the cell pellets were kept on ice and inactivated by ultraviolet light using a Vilber-Lourmat BLX312 UV crosslinker. For TEM preparation, samples were mixed with 20% (w/v) BSA and high-pressure-frozen with an HPM 010 (BAL-TEC) in 200 μm HPF carriers (Baltic Präparation). Freeze substitution (FS) was performed in acetone containing 1% (w/v) osmium tetroxide and 0.1% (w/v) uranyl acetate (12 h at −90 °C, 8 h at −60 °C, 8 h at −30 °C) using the FSU 010 (BAL-TEC). After FS, samples were infiltrated and embedded in Lowicryl HM20 (Polysciences) at −4 °C. Polymerisation was carried out with UV light. For ultrathin sectioning (60 nm), an ultramicrotome (Leica Ultracut E; Leica Biosystems) was used. After mounting on filmed copper grids and post-staining with lead citrate, the sections were studied in a transmission electron microscope (EM 902 A; ZEISS) at 80 kV. Images were acquired with a 1k FastScan CCD camera (TVIPS).

Isolation of *C. albicans* cell walls and acid hydrolysis

For cell wall isolation and preparation, overnight cultures (YEPD broth, 30 °C, 180 rpm) of wildtype (SC5314) and *och1* mutant *C. albicans* cells were diluted 1:50 in YEPD and incubated for 4 h at 30 °C and 180 rpm. After centrifugation (2000 × *g*, 1 min), the pellet was washed in PBS and the cell concentration was adjusted to 2.5×10^8/mL in SD broth. For each condition, 196 mL of media were inoculated with 4 mL of the adjusted exponential phase *C. albicans* cells. For the antifungal compounds, sub-inhibitory concentrations were used, *i.e.*, 128 μg/mL polymer LH or poly-HEA, 4 μg/mL tunicamycin, or 0.06 μg/mL caspofungin. After 6 h incubation at 30 °C with shaking at 180 rpm, cell walls were extracted according to an established protocol[95]. Briefly, the cells were disrupted by mechanical disruption with acid-washed glass beads. Samples were then washed five times with 1 M NaCl and cell walls were extracted using SDS-mercaptoethanol-buffer (50 mM Tris, 2% SDS, 0.3 M β-mercaptoethanol, 1 mM EDTA; pH 8.0) at 100 °C for 10 min. Cell wall pellets were resuspended in sterile double-distilled water, freeze-dried, and the dry weight of recovered cell walls was measured. Cell walls were resuspended in 100 μL 2 M TFA per mg dry weight, heated at 100 °C for 3 h, and supernatants were evaporated. The acid-hydrolysed walls were resuspended in 1 mL double-distilled water and evaporated at 70 °C twice. Samples were resuspended at a concentration of 10 mg/mL in water and stored at −20 °C.

Cell wall monosaccharide analysis

Before quantification by HPLC, the monosaccharides obtained *via* acid hydrolysis of *C. albicans* cell walls were derivatised following a previously described protocol[96]. Briefly, 100 μL of each sample was vigorously mixed with 100 μL of 0.3 M NaOH and 100 μL of 0.5 M 1-phenyl-3-methyl-5-pyrazolone(PMP)-methanol for 1 min, and incubated at 70 °C for 120 min. Samples were cooled to room temperature, and neutralised by the addition of 100 μL of 0.3 M HCl. To remove the residual PMP, 1 mL of chloroform was added, and the solutions were gently mixed. The lower chloroform phase was removed. This procedure was repeated twice. Solution cleanup was performed by solid phase extraction using C18 cartridges (Chromabond, 500 mg). The cartridges were conditioned with 1 mL of acetonitrile, followed by 1 mL of mobile phase solution (water:-acetonitrile 1:1 (v/v) with 0.025% of formic acid), followed by 1 mL of distilled water. The samples were loaded into the cartridge and washed with 1 mL distilled water twice, followed by 1 mL of chloroform. The monosaccharide-PMP derivatives were eluted with 1 mL of mobile phase. References of D(+)-mannose, D(+)-glucose, and D(+)-glucosamine (HPLC-grade, Sigma-Aldrich), the respective monomers of the fungal cell wall polysaccharides mannan, glucan, and chitin, were dissolved in distilled water a concentration of 500 μg/mL. The solutions were passed through a Chromafil PET-45/25 filter and derivatised as described above.

The monosaccharide-PMP derivatives were analysed by HPLC with an Agilent 1260 Infinity instrument with a photometric diode array, using a C8 column (Eclipse XDB, 5 μM, 4.6 × 150 mm). The mobile phase consisted of A: water with 0.1% formic acid, and B: acetonitrile. The solvent gradient started with 9:1 (A:B) for 2 min and was increased over 20 min to 100% B (flow rate 1 mL/min).

Hypha formation assay

To study the formation of hyphae and microcolonies by *C. albicans*, the cell concentration of a PBS-washed overnight culture was adjusted to 6×10^4/mL (4 and 6 h timepoints) and 400/mL (24 h timepoint) in RPMI-1640 (with L-glutamine, without phenol red). In a 24-well plate, 500 μL of RPMI-1640 medium plus LP (64 μg/mL final concentration), LH (16 μg/mL for 4 and 6 h timepoint, 4 μg/mL for 24 h timepoint), CB (32 μg/mL), or CX (32 μg/mL) were prepared. To this, 500 μL of diluted *C. albicans* suspension was added and the plates were incubated for 2, 4, or 24 h at 37 °C with 5% CO_2 in a humidified chamber to induce the formation of hyphae and microcolonies. After 2, 4, or 24 h, cells were fixed with formaldehyde (approx. 10% (v/v) final concentration from a 37% stock). The plates were then stored until imaging at 4 °C. Fixed cells were imaged using a ZEISS Axio Vert A1 microscope, equipped with a plan-apochromat 10× objective, AxioCam ICc1, and a 0.63× camera adaptor. The internal ZEN blue software was used to measure the length of 50 hyphae and diameters of 50 microcolonies per sample. The experiment was performed independently in triplicates.

Fungal clearance by macrophages

Human peripheral blood mononuclear cells (PBMCs) and monocytes were isolated from buffycoats donated by healthy volunteers. Isolation of PBMCs was performed by density gradient centrifugation over Lymphocytes Separation Medium (Capricorn Scientific) in a sterile 50 mL tube. CD14+ monocytes were selected from the PBMC fraction using magnetic beads and automated cell sorting (autoMACs; MiltenyiBiotec). To differentiate monocytes into monocyte-derived macrophages (MDMs), 1×10^7 cells were seeded into 175 cm^2 cell culture flasks in RPMI-1640 media with 2 mM L-glutamine (Thermo Fisher Scientific) containing 10% heat-inactivated foetal bovine serum (FBS; Bio&SELL) and 50 ng/mL recombinant human macrophage colony-stimulating factor (ImmunoTools) and incubated for seven days at 37 °C with 5% CO_2. Adherent MDMs were detached with 50 mM EDTA in PBS, seeded in 96-well plates at a concentration of 4×10^4 cells/well and incubated for 24 h in RPMI-1640 at 37 °C with 5% CO_2. Drug-dilution plates (120 μL per well) were prepared on the day of the experiment at two times final concentration of polymer LH, caspofungin, fluconazole and their respective combinations in RPMI-1640. An overnight culture of *C. albicans ADH1*-GFP (derived from SC5314), expressing GFP intracellularly, was centrifuged at 2500 × *g* for 1 min and the pellet was washed in PBS twice. GFP-expressing *C. albicans* has been chosen for this assay to facilitate the distinction of yeast and macrophages. The washed *C. albicans* cell culture was adjusted to a concentration of 1.2×10^6 cells/mL in RPMI-1640. 120 μL of the adjusted and washed cell suspension was added to each well of the prewarmed drug-dilution plate and incubated for 1 h at 30 °C in a humidified chamber. Samples for each donor were prepared in duplicates. In addition to the infected samples, uninfected samples were prepared in the same manner by replacing the *C. albicans* solution with RPMI-1640 medium. Afterward, the supernatant of the 96-well plates harbouring the macrophages was aspirated, and 200 μL of the pre-treated *C. albicans* cells in RPMI-1640, supplemented with the respective antifungal compounds, was added to the macrophages. The 96-well plates were centrifuged for 5 min at 200 × *g* to settle the cells for subsequent imaging. Following centrifugation, the 96-well plate was immediately transferred into a ZEISS Celldiscoverer 7 and incubated for 45 min at 37 °C and 5% CO_2. Images were acquired every 15 min using a 20× plan-apochromat objective at 2× magnification and fluorescence signal of GFP-expressing *C. albicans* was detected (LED excitation at 470 nm for 500 ms, 501–547 nm emission filter). ZEN software (version 3.1, blue edition) was used to analyse the images. Non-phagocytosed cells were counted at time 0 (set to 100%) and timepoint 15 min or 30 min (displayed relative to the count at time 0). The analysed timepoint was chosen based on when in the untreated controls non-phagocytosed *C. albicans* cells decreased to 30–50%, compared to time 0. A total of six donors were investigated on three different days.

Response of human peripheral blood mononuclear cells (PBMCs)

Human PBMCs were isolated from fresh human blood as described above and seeded in 96-well plates at 1×10^6 cells/well in 100 μL. The drug dilutions were prepared in RPMI-1640 medium at two-fold final concentration (150 μL each well for 2 donors) in a separate 96-well plate and prewarmed at 30 °C. A washed *C. albicans* overnight culture was diluted to 10^7 cells/mL in RPMI-1640. 150 μL of the adjusted *C. albicans* suspension was added to the wells of the drug-dilution plate and incubated for 1 h. In parallel, uninfected samples were prepared in the same manner by replacing *C. albicans* in RPMI-1640 by medium only to check the putative responses of the PBMCs to the antifungal compounds only. The seeded PBMCs were stimulated with 100 μL of the LH and RPMI pre-treated *C. albicans* samples and incubated for 24 h at 37 °C with 5% CO_2 in a humidified chamber. Afterwards, the 96-well plates were centrifuged at 250 × *g* for 10 min and 150 μL supernatant was collected and stored at −20 °C. Cytokine levels were detected by enzyme-linked immunosorbent assays (ELISA, R&D Systems) and were performed according to the protocol supplied by the manufacturer. Cytokine release was displayed relative to the untreated *C. albicans* control (set to 1) as fold changes. A total of 11 (IL-6 and IL-1β) or 8 donors (TNF) were analysed on 3 or 4 different days.

In vitro human epithelial cell infection model

To mimic human epithelial cells, A-431 epithelial cells (ACC 91)[97] were used. A-431 cells were derived from a vulva epidermoid carcinoma and are routinely used to simulate the vaginal mucosa[74,75,97,98]. The cells were cultivated in RPMI-1640 medium supplemented with 10% FBS in a humidified incubator at 37 °C with 5% CO_2 and regularly tested for *Mycoplasma* contamination. For seeding in 96-well plates, 200 μL of a 10^5 cells/mL suspension was added per well in RPMI-1640 medium, supplemented with 10% FBS. The plates were incubated for 48 h at 37 °C with 5% CO_2 in a humidified chamber to let the cells attach to the surface. On the day of infection, a washed *C. albicans* SC5314 overnight culture was diluted to 3.64×10^5 cells/mL in prewarmed RPMI-1640 medium (without FBS). A drug-dilution plate containing 110 μL 2× concentrated antifungal compound(s) was prepared as described in the MIC assay and prewarmed. The supernatants were aspirated from the seeded vaginal epithelial cells and 100 μL of the antifungal-*C. albicans* solutions in RPMI-1640 and 100 μL of the antifungal drug in RPMI-1640 were added with minimum preincubation time to infect the vaginal epithelial cells. As a control, an uninfected plate was prepared as described above without the addition of *C. albicans* (replaced by 100 μL of RPMI-1640). Infected and uninfected samples were incubated for 24 h at 37 °C and 5% CO_2 in a humidified chamber. Cells were stained with propidium iodide (1 μg/mL final concentration, 1 mg/mL stock) for 15 min at 37 °C with 5% CO_2 to detect damaged vaginal epithelial cells. The stained samples were imaged using a ZEISS Celldiscoverer 7 (5× plan-apochromat objective, 2× magnification, equipped with an Axiocam 506, prewarmed to 37 °C with 5% CO_2) for brightfield image acquisition (automatic exposure time and focus) and detection of fluorescence (LED excitation at 545 nm, 583–601 nm emission filter). To quantify damage caused by *C. albicans* to the vaginal epithelial cells,

lactate dehydrogenase (LDH), released by the epithelial cells, was measured in the supernatant. For that, Triton X-100 was added to at least two wells containing vaginal epithelial cells in medium at a final concentration of 0.1% from a 5–10% stock and incubated for 5 min at 37 °C with 5% CO_2, reflecting 100% damage to uninfected epithelial cells. Plates were centrifuged at 250 × *g* for 10 min, and 20 μL from the supernatants were taken up in 80 μL PBS and an LDH detection assay was performed using the Cytotoxicity Detection Kit (LDH) (Roche) following the manual's instructions. LDH release data is presented relative to the respective controls, *i.e.*, *C. albicans*-infected vaginal epithelial cells served as a control for the infected samples (set to 100%), and uninfected vaginal epithelial cells, treated with Triton X-100, were set to 100% for all uninfected samples. Uninfected, untreated vaginal epithelial cells were used as background controls and were subtracted from all measured values. All experiments were carried out independently at least in triplicates.

G. mellonella in vivo toxicity assay

The acute toxicity of AmpB, caspofungin, and polymer LH was tested in vivo in a *G. mellonella* model using previously described methods with slight modifications[79,99]. Briefly, *G. mellonella* larvae were originally obtained from Westmead hospital (Sydney, Australia) and maintained in an environmentally controlled room at Macquarie University (Sydney, Australia) at 30 °C and 65% humidity with a 12 h light/dark cycle. Larvae (200–250 mg) were individually injected with 10 μL of the respective compound into the last right proleg using a 100 μL syringe (Hamilton Ltd.), reaching final concentrations of 100 mg/kg (AmpB, caspofungin) or 250–500 mg/kg (polymer LH). For each condition, four larvae were treated, including a 1% (v/v) DMSO control (as the AmpB stock used DMSO as a solvent) or water (solvent for all dilutions of the compounds). Following injection, the larvae were incubated at 37 °C and monitored every 24 h for 10 days. Larval performance was assessed according to the *G. mellonella* Health Index Scoring System[100].

G. mellonella-C. albicans infection model

Before infection, *C. albicans* SC5314 was cultured on YEPD agar plates and grown overnight in YEPD broth at 30 °C and 200 rpm. An aliquot of the culture was then washed twice in PBS and counted using a haemocytometer. Fungal cell viability was ascertained by backplating.

To test the in vivo efficacy of caspofungin, polymer LH and the combination of both to prevent infection by *C. albicans*, *Galleria* larvae (200 − 250 mg) were infected with 1×10^5 *C. albicans* cells/larva suspended in 10 μL of water in the last right proleg and incubated at 37 °C. After 2 h, 10 μL of the tested compounds or compound combinations were injected in the last left proleg. Three groups of larvae were included as controls: infected larvae treated with 100 mg/kg caspofungin as a positive treatment control, infected larvae injected with water only as a negative treatment control, and uninfected larvae injected with water to control for injection injury. Larval survival was monitored daily over 14 days. The experiment was performed in three biological replicates, whereby each condition was tested in 6–7 larvae per replicate ($n = 19$ total). Statistical analyses were performed using IBM SPSS Statistics 29.0.

Evolution assay

For the in vitro evolution assay, *C. albicans* SC5314 cells were incubated and prepared as in the MIC assays in the presence of polymer LH (32 μg/mL), the synergistic combinations of LH (4 μg/mL) with caspofungin (0.07 μg/mL) or fluconazole (0.13 μg/mL), and the antifungal drugs fluconazole (0.5 μg/mL) and caspofungin (0.5 μg/mL) alone as controls. All samples, including an untreated control, were prepared in four replicates in a 96-well plate. After 24 h incubation at 35 °C, fungal growth was measured photometrically (absorbance measurement at 405 nm with a Tecan infinite M200 plate reader) and compared to the untreated control. After the first day, growth was inhibited in all samples except the untreated control, resulting in an absorption <0.1, and continued cell viability was assured *via* backplating on YEPD plates. In case of a measured increase in absorbance indicating fungal growth after day 1, the samples were diluted based on their absorption: absorption >0.5 (indicating $>5 \times 10^7$ cells/mL) samples were diluted 1:1000; absorption between 0.2 and 0.5 ($>10^7$ cells/mL) samples were diluted 1:500; absorption between 0.1 and 0.2 ($>10^6$ cells/mL) samples were diluted 1:100. Absorptions below 0.1 were defined as "no visual growth" and further used undiluted. A sample of 20 μL of diluted or undiluted cell cultures was added to 180 μL of fresh medium, plus respective antifungal. This procedure was repeated for 14 consecutive days.

Afterwards, 50 μL were incubated in 450 μL modified RPMI medium containing the antifungal at a concentration of 2× MIC in Eppendorf tubes under gentle rolling at 35 °C. If growth was observed after 24 h or 48 h, a sample was plated on YEPD and 500 μL of 50% (v/v) glycerol was added to the more tolerant fungal cells and frozen at −80 °C. If no growth was observed after 48 h, the sample was considered not more tolerant to the respective antifungal. A *C. albicans* MIC assay for the polymers LP, LH, CB and CX, and the antifungal compounds AmpB, fluconazole, caspofungin and tunicamycin, was performed with the more tolerant strains.

The most tolerant strains were selected for whole genome sequencing. Genomic DNA was isolated from overnight cultures of evolved strains by phenol/chloroform extraction as described in ref. 101. Whole genome sequencing of the evolved strains was performed on an Illumina Novaseq, 2 × 150 bp sequencing and 10 million raw paired-end reads per sample by Azenta Life Sciences. The sequences were trimmed with Trimmomatic (v0.40) and aligned to *C. albicans* assembly 22 using Bowtie2 (v2.4) with standard settings. The lab strain (SC5314) used for the evolution experiment was also sequenced and assembled. Genomic variants unique to an evolved strain were called with SnpEff (v5.1)[102]. Changes in ploidy, loss of heterozygosity and copy number variation were determined by YMAP[103]. For each strain, the read depth for each nucleotide was determined without any filters using samtools (samtools depth – aa, version 1.15.1)[104] on galaxyproject.org. For each evolved strain the relative copy number (to lab strain SC5314 $t = 0$ strain) was estimated by calculating the sequencing depth for every 500 bp window normalised to the average whole genome coverage, using R[105] (method described in refs. 106,107). Integrative genomics viewer[108] and R (package Gviz[109]) were used to visualise genome coverage for genomic and copy number variants.

Statistics and reproducibility

Statistical analyses were performed with GraphPad Prism v10.1 using the methods indicated in each figure legend. Sample sizes were chosen according to previous experience for the expected effect sizes, and no statistical method was used to predetermine sample size. All attempts at replication were successful and no data were excluded from the analyses. Data is shown as mean with standard deviation (SD), unless specifically indicated otherwise.

Reporting summary

Further information on research design is available in the Nature Portfolio Reporting Summary linked to this article.

Data availability

The whole genome sequencing data generated in this study have been deposited in the European Nucleotide Archive database under accession code PRJEB65085. The microarray data generated in this study

have been deposited in the ArrayExpress database under accession code E-MTAB-13294. Source data are provided with this paper.

References

1. Clark, C. & Drummond, R. A. The hidden cost of modern medical interventions: How medical advances have shaped the prevalence of human fungal disease. *Pathogens* **8**, 45 (2019).
2. Perfect, J. R., Hachem, R. & Wingard, J. R. Update on epidemiology of and preventive strategies for invasive fungal infections in cancer patients. *Clin. Infect. Dis.* **59**, S352–S355 (2014).
3. Brown, G. D. et al. Hidden killers: Human fungal infections. *Sci. Transl. Med.* **4**, 165rv113 (2012).
4. Hoenigl, M. et al. COVID-19-associated fungal infections. *Nat. Microbiol* **7**, 1127–1140 (2022).
5. Mazi, P. B. et al. Attributable mortality of *Candida* bloodstream infections in the modern era: a propensity score analysis. *Clin. Infect. Dis.* **75**, 1031–1036 (2022).
6. Pfaller, M. A., Diekema, D. J., Turnidge, J. D., Castanheira, M. & Jones, R. N. Twenty years of the SENTRY antifungal surveillance program: results for *Candida* species from 1997-2016. *Open Forum Infect. Dis.* **6**, S79–S94 (2019).
7. Nnadi, N. E. & Carter, D. A. Climate change and the emergence of fungal pathogens. *PLoS Pathog.* **17**, e1009503 (2021).
8. Casadevall, A., Climate change. brings the specter of new infectious diseases. *J. Clin. Invest.* **130**, 553–555 (2020).
9. WHO. *WHO Fungal Priority Pathogens List to Guide Research, Development and Public Health Action* (World Health Organization, 2022).
10. Perfect, J. R. The antifungal pipeline: a reality check. *Nat. Rev. Drug Discov.* **16**, 603–616 (2017).
11. Revie, N. M., Iyer, K. R., Robbins, N. & Cowen, L. E. Antifungal drug resistance: Evolution, mechanisms and impact. *Curr. Opin. Microbiol.* **45**, 70–76 (2018).
12. CDC. *Antibiotic Resistance Threats in the United States, 2019* (U. S. Department of Health and Human Services, CDC, accessed 12 Mar 2024); https://www.cdc.gov/drugresistance/pdf/threats-report/2019-ar-threats-report-508.pdf.
13. Gintjee, T. J., Donnelley, M. A. & Thompson, G. R. Aspiring antifungals: Review of current antifungal pipeline developments. *J. Fungi* **6**, 28 (2020).
14. Hoenigl, M. et al. The antifungal pipeline: fosmanogepix, ibrexafungerp, olorofim, opelconazole, and rezafungin. *Drugs* **81**, 1703–1729 (2021).
15. Pappas, P. G. et al. Clinical safety and efficacy of novel antifungal, fosmanogepix, for the treatment of candidaemia: results from a Phase 2 trial. *J. Antimicrob. Chemother.* **78**, 2471–2480 (2023).
16. Spitzer, M., Robbins, N. & Wright, G. D. Combinatorial strategies for combating invasive fungal infections. *Virulence* **8**, 169–185 (2017).
17. Revie, N. M. et al. Targeting fungal membrane homeostasis with imidazopyrazoindoles impairs azole resistance and biofilm formation. *Nat. Commun.* **13**, 3634 (2022).
18. dos Reis, T. F. et al. A host defense peptide mimetic, brilacidin, potentiates caspofungin antifungal activity against human pathogenic fungi. *Nat. Commun.* **14**, 2052 (2023).
19. Fernández de Ullivarri, M., Arbulu, S., Garcia-Gutierrez, E. & Cotter, P. D. Antifungal peptides as therapeutic agents. *Front. Cell Infect. Microbiol.* **10**, 00105 (2020).
20. Jung, K., Corrigan, N., Wong, E. H. H. & Boyer, C. Bioactive synthetic polymers. *Adv. Mater.* **34**, 2105063 (2022).
21. Jiang, W., Wu, Y., Zhou, M., Song, G. & Liu, R. Advance and designing strategies in polymeric antifungal agents inspired by membrane-active peptides. *Chem. Eur. J.* **28**, e202202226 (2022).
22. Liu, R. et al. Nylon-3 polymers with selective antifungal activity. *J. Am. Chem. Soc.* **135**, 5270–5273 (2013).
23. Zhang, D. et al. Microbial metabolite inspired β-peptide polymers displaying potent and selective antifungal activity. *Adv. Sci.* **9**, 2104871 (2022).
24. Jiang, W. et al. Short guanidinium-functionalized poly(2-oxazoline) s displaying potent therapeutic efficacy on drug-resistant fungal infections. *Angew. Chem. Int. Ed.* **61**, e202200778 (2022).
25. Jiang, W. et al. Peptide-mimicking poly(2-oxazoline)s possessing potent antifungal activity and BBB penetrating property to treat invasive infections and meningitis. *J. Am. Chem. Soc.* **145**, 25753–25765 (2023).
26. Ng, V. W. L. et al. Antimicrobial polycarbonates: Investigating the impact of nitrogen-containing heterocycles as quaternizing agents. *Macromolecules* **47**, 1285–1291 (2014).
27. Schaefer, S. et al. Rational design of an antifungal polyacrylamide library with reduced host-cell toxicity. *ACS Appl. Mater. Interfaces* **13**, 27430–27444 (2021).
28. Schaefer, S. et al. Mimicking charged host-defense peptides to tune the antifungal activity and biocompatibility of amphiphilic polymers. *Biomacromolecules* **25**, 871–889 (2024).
29. Li, P. et al. Cationic peptidopolysaccharides show excellent broad-spectrum antimicrobial activities and high selectivity. *Adv. Mater.* **24**, 4130–4137 (2012).
30. Corrigan, N. et al. Reversible-deactivation radical polymerization (controlled/living radical polymerization): from discovery to materials design and applications. *Prog. Polym. Sci.* **111**, 101311 (2020).
31. Lutz, J.-F. Defining the field of sequence-controlled polymers. *Macromol. Rapid Commun.* **38**, 1700582 (2017).
32. CLSI. *Performance Standards for Antifungal Susceptibility Testing of Yeasts*, 1st edn (Clinical and Laboratory Standards Institute, Wayne, PA, 2017).
33. CLSI. *Reference Method for Broth Dilution Antifungal Susceptibility Testing of Yeasts*, 4th edn (Clinical and Laboratory Standards Institute, Wayne, PA, 2017).
34. Lackner, M. et al. Positions and numbers of *FKS* mutations in *Candida albicans* selectively influence in vitro and in vivo susceptibilities to echinocandin treatment. *Antimicrob. Agents Chemother.* **58**, 3626–3635 (2014).
35. Martel, C. M. et al. A clinical isolate of *Candida albicans* with mutations in *ERG11* (encoding sterol 14α-demethylase) and *ERG5* (encoding C22 desaturase) is cross resistant to azoles and amphotericin B. *Antimicrob. Agents Chemother.* **54**, 3578–3583 (2010).
36. Martel, C. M. et al. Identification and characterization of four azole-resistant *erg3* mutants of *Candida albicans*. *Antimicrob. Agents Chemother.* **54**, 4527–4533 (2010).
37. Fischer, D. et al. Disruption of membrane integrity by the bacterium-derived antifungal jagaricin. *Antimicrob. Agents Chemother.* **63**, e00707–e00719 (2019).
38. Durnaś, B. et al. Candidacidal activity of selected ceragenins and human cathelicidin LL-37 in experimental settings mimicking infection sites. *PLoS ONE* **11**, e0157242 (2016).
39. Yang, Y. et al. A novel dual-targeted α-helical peptide with potent antifungal activity against fluconazole-resistant *Candida albicans* clinical isolates. *Front. Microbiol.* **11**, 548620 (2020).
40. Rothstein, D. M. et al. Anticandida activity is retained in P-113, a 12-amino-acid fragment of histatin 5. *Antimicrob. Agents Chemother.* **45**, 1367–1373 (2001).
41. Han, J., Jyoti, M. A., Song, H.-Y. & Jang, W. S. Antifungal activity and action mechanism of histatin 5-halocidin hybrid peptides against *Candida ssp*. *PLoS ONE* **11**, e0150196 (2016).
42. Wubulikasimu, A., Huang, Y., Wali, A., Yili, A. & Rong, M. A designed antifungal peptide with therapeutic potential for clinical drug-resistant *Candida albicans*. *Biochem. Biophys. Res. Commun.* **533**, 404–409 (2020).

43. Hong, S. Y., Oh, J. E. & Lee, K. H. In vitro antifungal activity and cytotoxicity of a novel membrane-active peptide. *Antimicrob. Agents Chemother.* **43**, 1704–1707 (1999).
44. Ordonez, S. R., Amarullah, I. H., Wubbolts, R. W., Veldhuizen, E. J. A. & Haagsman, H. P. Fungicidal mechanisms of cathelicidins LL-37 and CATH-2 revealed by live-cell imaging. *Antimicrob. Agents Chemother.* **58**, 2240–2248 (2014).
45. Boyle, E. I. et al. GO::TermFinder—open source software for accessing gene ontology information and finding significantly enriched gene ontology terms associated with a list of genes. *Bioinformatics* **20**, 3710–3715 (2004).
46. Kanehisa, M. & Goto, S. KEGG: Kyoto Encyclopedia of Genes and Genomes. *Nucleic Acids Res.* **28**, 27–30 (2000).
47. Kanehisa, M., Furumichi, M., Sato, Y., Kawashima, M. & Ishiguro-Watanabe, M. KEGG for taxonomy-based analysis of pathways and genomes. *Nucleic Acids Res.* **51**, D587–D592 (2022).
48. Schaeffer, H. J. & Weber, M. J. Mitogen-activated protein kinases: Specific messages from ubiquitous messengers. *Mol. Cell. Biol.* **19**, 2435–2444 (1999).
49. Monge, R. A., Román, E., Nombela, C. & Pla, J. The MAP kinase signal transduction network in *Candida albicans*. *Microbiology* **152**, 905–912 (2006).
50. Liu, T. T. et al. Genome-wide expression profiling of the response to azole, polyene, echinocandin, and pyrimidine antifungal agents in *Candida albicans*. *Antimicrob. Agents Chemother.* **49**, 2226–2236 (2005).
51. Rautenbach, M., Troskie, A. M. & Vosloo, J. A. Antifungal peptides: to be or not to be membrane active. *Biochimie* **130**, 132–145 (2016).
52. Wang, T. et al. Transcriptional responses of *Candida albicans* to antimicrobial peptide MAF-1A. *Front. Microbiol.* **8**, 894 (2017).
53. Graupner, K. et al. Imaging mass spectrometry and genome mining reveal highly antifungal virulence factor of mushroom soft rot pathogen. *Angew. Chem. Int. Ed.* **51**, 13173–13177 (2012).
54. Sircaik, S. et al. The protein kinase Ire1 impacts pathogenicity of *Candida albicans* by regulating homeostatic adaptation to endoplasmic reticulum stress. *Cell Microbiol.* **23**, e13307 (2021).
55. Badrane, H. et al. The *Candida albicans* phosphatase Inp51p interacts with the EH domain protein Irs4p, regulates phosphatidylinositol-4,5-bisphosphate levels and influences hyphal formation, the cell integrity pathway and virulence. *Microbiology* **154**, 3296–3308 (2008).
56. Hall, R. A. & Gow, N. A. R. Mannosylation in *Candida albicans*: role in cell wall function and immune recognition. *Mol. Microbiol.* **90**, 1147–1161 (2013).
57. Rispail, N. et al. Comparative genomics of MAP kinase and calcium–calcineurin signalling components in plant and human pathogenic fungi. *Fungal Genet. Biol.* **46**, 287–298 (2009).
58. Mayer, F. L. et al. The novel *Candida albicans* transporter Dur31 is a multi-stage pathogenicity factor. *PLoS Pathog.* **8**, e1002592 (2012).
59. Kumar, R. et al. Histatin 5 uptake by *Candida albicans* utilizes polyamine transporters Dur3 and Dur31 proteins. *J. Biol. Chem.* **286**, 43748–43758 (2011).
60. Cesare, G. B. D., Cristy, S. A., Garsin, D. A., Lorenz, M. C. & Alspaugh, J. A. Antimicrobial peptides: a new frontier in antifungal therapy. *mBio* **11**, e02123–02120 (2020).
61. Gray, K. C. et al. Amphotericin primarily kills yeast by simply binding ergosterol. *Proc. Natl Acad. Sci. USA* **109**, 2234–2239 (2012).
62. Anderson, T. M. et al. Amphotericin forms an extramembranous and fungicidal sterol sponge. *Nat. Chem. Biol.* **10**, 400–406 (2014).
63. Kuo, S. C. & Lampen, J. O. Tunicamycin — an inhibitor of yeast glycoprotein synthesis. *Biochem. Biophys. Res. Commun.* **58**, 287–295 (1974).
64. Lenardon, M. D., Sood, P., Dorfmueller, H. C., Brown, A. J. P. & Gow, N. A. R. Scalar nanostructure of the *Candida albicans* cell wall; a molecular, cellular and ultrastructural analysis and interpretation. *Cell Surf.* **6**, 100047 (2020).
65. Gow, N. A. R. & Hube, B. Importance of the *Candida albicans* cell wall during commensalism and infection. *Curr. Opin. Microbiol.* **15**, 406–412 (2012).
66. McKenzie, C. G. et al. Contribution of *Candida albicans* cell wall components to recognition by and escape from murine macrophages. *Infect. Immun.* **78**, 1650–1658 (2010).
67. Bain, J. M. et al. *Candida albicans* hypha formation and mannan masking of β-glucan inhibit macrophage phagosome maturation. *mBio* **5**, e01874–01814 (2014).
68. Yadav, B. et al. Differences in fungal immune recognition by monocytes and macrophages: N-mannan can be a shield or activator of immune recognition. *Cell Surf.* **6**, 100042 (2020).
69. Jiang, H.-H. et al. Cell wall mannoprotein of *Candida albicans* polarizes macrophages and affects proliferation and apoptosis through activation of the Akt signal pathway. *Int. Immunopharmacol.* **72**, 308–321 (2019).
70. Gow, N. A. R., Brown, A. J. P. & Odds, F. C. Fungal morphogenesis and host invasion. *Curr. Opin. Microbiol.* **5**, 366–371 (2002).
71. Sprague, J. L., Kasper, L. & Hube, B. From intestinal colonization to systemic infections: *Candida albicans* translocation and dissemination. *Gut Microbes* **14**, 2154548 (2022).
72. Denning, D. W., Kneale, M., Sobel, J. D. & Rautemaa-Richardson, R. Global burden of recurrent vulvovaginal candidiasis: a systematic review. *Lancet Infect. Dis.* **18**, e339–e347 (2018).
73. Sobel, J. D. Vulvovaginal candidosis. *Lancet* **369**, 1961–1971 (2007).
74. Hernandez, R. & Rupp, S. in *Host-Pathogen Interactions: Methods and Protocols* (eds Rupp, S. & Sohn, K.) 105–123 (Humana Press, Totowa, NJ, 2009).
75. Schaller, M., Zakikhany, K., Naglik, J. R., Weindl, G. & Hube, B. Models of oral and vaginal candidiasis based on in vitro reconstituted human epithelia. *Nat. Protoc.* **1**, 2767–2773 (2006).
76. Jacobsen, I. D. *Galleria mellonella* as a model host to study virulence of *Candida*. *Virulence* **5**, 237–239 (2014).
77. Gu, W., Yu, Q., Yu, C. & Sun, S. In vivo activity of fluconazole/tetracycline combinations in *Galleria mellonella* with resistant *Candida albicans*. *Infect. J. Glob. Antimicrob. Resist.* **13**, 74–80 (2018).
78. Li, D.-D. et al. Using *Galleria mellonella-Candida albicans* infection model to evaluate antifungal agents. *Biol. Pharm. Bull.* **36**, 1482–1487 (2013).
79. Frei, A. et al. Metal complexes as antifungals? From a crowdsourced compound library to the first in vivo experiments. *JACS Au* **2**, 2277–2294 (2022).
80. Berman, J. & Krysan, D. J. Drug resistance and tolerance in fungi. *Nat. Rev. Microbiol.* **18**, 319–331 (2020).
81. Selmecki, A., Forche, A. & Berman, J. Aneuploidy and isochromosome formation in drug-resistant *Candida albicans*. *Science* **313**, 367–370 (2006).
82. Yang, F. et al. The fitness costs and benefits of trisomy of each *Candida albicans* chromosome. *Genetics* **218**, iyab056 (2021).
83. Selmecki, A., Gerami-Nejad, M., Paulson, C., Forche, A. & Berman, J. An isochromosome confers drug resistance in vivo by amplification of two genes, *ERG11* and *TAC1*. *Mol. Microbiol.* **68**, 624–641 (2008).
84. Yang, F. et al. Tunicamycin potentiates antifungal drug tolerance *via* aneuploidy in *Candida albicans*. *mBio* **12**, e02272–02221 (2021).

85. Wei, M.-X. et al. Enantioselective synthesis of *Amaryllidaceae* alkaloids (+)-vittatine, (+)-*epi*-vittatine, and (+)-buphanisine. *Chem. Asian J.* **8**, 1966–1971 (2013).
86. Nguyen, T.-K. et al. Rational design of single-chain polymeric nanoparticles that kill planktonic and biofilm bacteria. *ACS Infect. Dis.* **3**, 237–248 (2017).
87. Phuong, P. T. et al. Effect of hydrophobic groups on antimicrobial and hemolytic activity: developing a predictive tool for ternary antimicrobial polymers. *Biomacromolecules* **21**, 5241–5255 (2020).
88. Judzewitsch, P. R., Zhao, L., Wong, E. H. H. & Boyer, C. High-throughput synthesis of antimicrobial copolymers and rapid evaluation of their bioactivity. *Macromolecules* **52**, 3975–3986 (2019).
89. Wächtler, B., Wilson, D., Haedicke, K., Dalle, F. & Hube, B. From attachment to damage: defined genes of *Candida albicans* mediate adhesion, invasion and damage during interaction with oral epithelial cells. *PLoS ONE* **6**, e17046 (2011).
90. Yu, G., Wang, L. G., Han, Y. & He, Q. Y. clusterProfiler: an R package for comparing biological themes among gene clusters. *OMICS* **16**, 284–287 (2012).
91. Wu, T. et al. clusterProfiler 4.0: a universal enrichment tool for interpreting omics data. *Innovation* **2**, 100141 (2021).
92. Schneider, C. A., Rasband, W. S. & Eliceiri, K. W. NIH Image to ImageJ: 25 years of image analysis. *Nat. Methods* **9**, 671–675 (2012).
93. Ejsing, C. S. et al. Global analysis of the yeast lipidome by quantitative shotgun mass spectrometry. *Proc. Natl Acad. Sci. USA* **106**, 2136–2141 (2009).
94. Rose, H. G. & Oklander, M. Improved procedure for the extraction of lipids from human erythrocytes. *J. Lipid Res.* **6**, 428–431 (1965).
95. Plaine, A. et al. Functional analysis of *Candida albicans* GPI-anchored proteins: roles in cell wall integrity and caspofungin sensitivity. *Fungal Genet. Biol.* **45**, 1404–1414 (2008).
96. Wang, W., Wang, Y., Chen, F. & Zheng, F. Comparison of determination of sugar-PMP derivatives by two different stationary phases and two HPLC detectors: C_{18} vs. amide columns and DAD vs. ELSD. *J. Food Compos Anal.* **96**, 103715 (2021).
97. Giard, D. J. et al. In vitro cultivation of human tumors: establishment of cell lines derived from a series of solid tumors. *J. Natl Cancer Inst.* **51**, 1417–1423 (1973).
98. Pekmezovic, M. et al. *Candida* pathogens induce protective mitochondria-associated type I interferon signalling and a damage-driven response in vaginal epithelial cells. *Nat. Microbiol.* **6**, 643–657 (2021).
99. Frei, A. et al. Platinum cyclooctadiene complexes with activity against Gram-positive bacteria. *ChemMedChem* **16**, 3165–3171 (2021).
100. Tsai, C. J.-Y., Loh, J. M. S. & Proft, T. *Galleria mellonella* infection models for the study of bacterial diseases and for antimicrobial drug testing. *Virulence* **7**, 214–229 (2016).
101. Siscar-Lewin, S. et al. Transient mitochondria dysfunction confers fungal cross-resistance against phagocytic killing and fluconazole. *mBio* **12**, e01128–01121 (2021).
102. Cingolani, P. et al. A program for annotating and predicting the effects of single nucleotide polymorphisms, SnpEff. *Fly* **6**, 80–92 (2012).
103. Abbey, D. A. et al. YMAP: a pipeline for visualization of copy number variation and loss of heterozygosity in eukaryotic pathogens. *Genome Med.* **6**, 100 (2014).
104. Danecek, P. et al. Twelve years of SAMtools and BCFtools. *GigaScience* **10**, giab008 (2021).
105. Zeileis, A. & Grothendieck, G. zoo: S3 infrastructure for regular and irregular time series. *J. Stat. Softw.* **14**, 1–27 (2005).
106. Todd, R. T. & Selmecki, A. Expandable and reversible copy number amplification drives rapid adaptation to antifungal drugs. *eLife* **9**, e58349 (2020).
107. Todd, R. T. & Selmecki, A. in Antifungal Drug Resistance: Methods and Protocols (eds Krysan, D. J. & Moye-Rowley, W. S.) 105–125 (Springer US, New York, NY, 2023).
108. Robinson, J. T. et al. Integrative genomics viewer. *Nat. Biotechnol.* **29**, 24–26 (2011).
109. Hahne, F. & Ivanek, R. in *Statistical Genomics* (eds Mathé, E. & Davis, S.) 335–351 (Springer New York, New York, NY, 2016).

Acknowledgements

S.B. is supported by the Priority Programm SPP2225 "Exit strategies of intracellular pathogens" of the German Research Foundation (Deutsche Forschungsgemeinschaft – DFG, project 446404928). R.V. has received funding from the AReST grant of the German Bundesministerium für Bildung und Forschung (BMBF, project 16GW0238K). S.A. was supported by funding from the European Union's Horizon 2020 research and innovation programme under grant agreement No 847507 (HDM-FUN). M.S.G. is supported by the Deutsche Forschungsgemeinschaft (DFG, German Research Foundation) Emmy Noether Program (project no. 434385622 / GR 5617/1-1). J.L.S. and M.S.G. were supported by the DFG within the Collaborative Research Centre (CRC)/Transregio (TRR) 124 "FungiNet" project C1 (DFG project number 210879364). E.S. would like to thank Electron Microscopy Centre in Jena for the support by providing the equipment for TEM preparation and evaluation. B.Q. would like to acknowledge the DFG project QU116/9-1 for funding. A.K.C. was supported by ARC Future Fellowship FT220100152. A.K.C. and H.D. acknowledge Macquarie University Research Infrastructure Scheme (MQRIS) grants for funding the *Galleria* Research Facility. P.R.J. acknowledges the receipt of an Australian Government Research Training Program Scholarship. S.S. is supported by a University International Postgraduate Award from the University of New South Wales (UNSW). C.B. would like to acknowledge ARC Laureate Fellowship (FL220100016) for funding. T.G. was supported by the DFG Priority Program 2225 "Exit Strategies of extracellular pathogens". C.H. and M.S.G. received funding from Germany's Excellence Strategy – EXC 2051 – Project-ID 390713860 ("Balance of the Microverse"). N.C. is a recipient of an Australian Research Council Discovery Early Career Researcher Award (DE240100917). We gratefully acknowledge financial support by the Deutsche Forschungsgemeinschaft (Leibniz Award to C.H.). The authors would like to thank the NMR facility within the Mark Wainwright Analytical Centre (MWAC) at UNSW for providing and maintenance of the necessary instruments; Eh Hau Pan for technical assistance at the School of Chemical Engineering at UNSW; Bernhard Hube (HKI Jena) for supporting S.S.'s research stay at HKI Jena and his valuable feedback on the project; Maximilian Himmel, Julia Mantke, and Stephanie Wisgott for technical assistance at the HKI Jena; Steffi Feller for assistance with organising S.S.'s research stay at the HKI in Jena; Osama Elshafee (HKI Jena) for providing the *ADH1*-GFP *C. albicans* strain; Stefanie Allert (HKI Jena) for providing cell membrane extracts; Marisa Valentine, Marina Pekmezović. and Sophia Hitzler (all HKI Jena) for providing A-431 cells.

Author contributions

S.S., R.V., J.L.S., S.A., H.D., P.R.J., S.M.L., T.L.S., and E.S. designed and performed the experiments. S.S., R.V., H.D., S.M.L., T.L.S., E.S., T.G., A.K.C., N.C., M.D.L., and S.B. analysed the data and created the figures. B.Q., C.H., K.S., T.G., A.K.C., N.C., M.S.G., C.B., M.D.L., S.B. supervised the project and helped in data analysis. S.S., R.V., C.B., M.D.L., and S.B. wrote the original draft. All authors have revised the manuscript and approved the submitted version.

Competing interests

The authors declare no competing interests.

Additional information

Supplementary information The online version contains supplementary material available at https://doi.org/10.1038/s41467-024-50491-x.

Correspondence and requests for materials should be addressed to Cyrille Boyer, Megan D. Lenardon or Sascha Brunke.

Peer review information *Nature Communications* thanks Dominique Sanglard and the other, anonymous, reviewer(s) for their contribution to the peer review of this work. A peer review file is available.

[1]School of Chemical Engineering, University of New South Wales (UNSW), Sydney, NSW, Australia. [2]Australian Centre for NanoMedicine, UNSW, Sydney, NSW, Australia. [3]School of Biotechnology and Biomolecular Sciences, UNSW, Sydney, NSW, Australia. [4]Department of Microbial Pathogenicity Mechanisms, Leibniz Institute for Natural Product Research and Infection Biology, Hans Knoell Institute, Jena, Germany. [5]ARC Centre of Excellence in Synthetic Biology, School of Natural Sciences, Macquarie University, North Ryde, NSW, Australia. [6]Division of Biophysics, Research Center Borstel, Leibniz Lung Center, Borstel, Germany. [7]Department of Biomolecular Chemistry, Leibniz Institute for Natural Product Research and Infection Biology, Hans Knoell Institute, Jena, Germany. [8]Institute of Biochemistry I, Jena University Hospital – Friedrich Schiller University Jena, Jena, Germany. [9]Faculty of Biological Sciences, Friedrich Schiller University Jena, Jena, Germany. [10]Cluster of Excellence Balance of the Microverse, Friedrich Schiller University Jena, Jena, Germany. [11]Centre for Structural Systems Biology (CSSB), Hamburg, Germany. [12]Junior Research Group Adaptive Pathogenicity Strategies, Leibniz Institute for Natural Product Research and Infection Biology, Hans Knoell Institute, Jena, Germany. ✉e-mail: cboyer@unsw.edu.au; m.lenardon@unsw.edu.au; sascha.brunke@leibniz-hki.de